The Abdus Salam
International Centre for Theoretical Physics

United Nations
Educational, Scientific and
Cultural Organization

IAEA
International Atomic Energy Agency

2141-16

Joint ICTP-IAEA Workshop on Nuclear Reaction Data for Advanced Reactor Technologies

3 - 14 May 2010

Statistical theory of nuclear reactions

IGNATYUK Anatoly
IPPE
Obninsk
RUSSIAN FEDERATION

Statistical theory of nuclear reactions

A.V.Ignatyuk,
Institute of Physics and Power Engineering, Obninsk, Russia

Abstract: Basic components of the statistical theory of nuclear reactions are reviewed in the lectures. The relations used for the analyses of resonance structure of neutron-induced reactions are briefly discussed. Special attention is spent to approximations requiered for a description of the cross sections averaged over resonances. Main nuclear models used in the analysis of various reaction channels are considered together with the corresponding experimental data. The sets of theoretical model parameters recommended for practical applications are briefly commented.

1 Resonance structure of neutron cross sections

Nuclear reactions induced by neutrons relate to the most studied nuclear processes. Intensive researches of neutron interaction with atomic nuclei have been going on over more than 70 years since the discovery of the neutron. Extensive experimental information about the neutron induced reactions has been collected which was very important for both the evolution of fundamental concepts of nuclear physics and development of nuclear power and nuclear technology.

Since the exploration of specific features of neutron induced reactions by the Fermi group [35A] their investigations have been developed by many laboratories and have resulted in the creation of fundamental concepts of nuclear reaction theory.

In order to explain observed strong changes of neutron reaction cross sections at narrow energy intervals, N.Bohr has proposed the model of compound nucleus [36B1]. In accordance with this model the excitation energy carried in a nucleus by the neutron shares out quickly enough over many nucleons. Because the probability of concentration on one nucleon of an essential part of the energy that is required for an escape from nucleus is rather small, the formed excited nucleus will exist during a significant time undergoing a myriad of collisions between nucleons until its decay occurs by the emission of a nucleon or electromagnetic radiation. The long lifetime of an excited nucleus permits to present the nuclear reaction as proceeding in two stages: the formation of the compound nucleus by the collision of the projectile with a target nucleus and the compound nucleus decay into possible pairs of reaction products. The hypothesis about the independence of a compound nucleus decay from its formation was used as the principal idea in many works devoted to the development of the nuclear reaction theory [36B2, 38K, 47W, 58L].

According to the formal theory of scattering the cross section of a nuclear reaction may be described by means of the scattering or *S*-matrix, the elements S_{ab} of which define the asymptotic amplitude of the outgoing wave in channel *b* induced by the plane wave of unit amplitude in channel *a* [52B2, 58L]. The cross section integrated over angles for the reaction *A(.a,b)B* can be written as

$$\sigma_{ab} = \pi\lambda\!\!\!^{-2}_a g_a \left|\delta_{ab} - S_{ab}\right|^2 \quad , \qquad (1.1)$$

where $\lambda\!\!\!^{-}_a$ is the length of a wave for the incoming channel; $g_a=(2J+1)/(2s_a+1)(2I_a+1)$ is the statistical weight factor connected with the total angular momentum *J* and the spins of the incident particle s_a and the target nucleus I_a . Here the subscripts *a* and *b* specify the complete set of quantum numbers needed for the description of the initial and final states of the projectile, the target, the reaction products and also their relative motion.

The important properties of *S*-matrix are its symmetry

$$S_{ab} = S_{ba} \quad , \qquad (1.2)$$

that reflects the invariance of the scattering system to time inversion, and its unitarity

$$\sum_b S_{ab} S^*_{cb} = \delta_{ac} \quad , \qquad (1.3)$$

reflecting the total flux conservation in the reaction.

Using (1.3), we can express the total interaction cross section σ_t and the total reaction cross section σ_r via the elements of the elastic scattering channel alone

$$\sigma_r = \sum_{b\neq a}\sigma_{ab} = \pi\lambda\!\!\!^{-2}_a g_a (1-|S_{aa}|^2) \quad ,$$
$$\sigma_t = \sum_{b}\sigma_{ab} = 2\pi\lambda\!\!\!^{-2}_a g_a (1-\mathrm{Re}\,S_{aa}) . \qquad (1.4)$$

If observed cross sections are formed by a superposition of many entrance and exit channels Eqs. (1.4) should be summed over nonfixed quantum characteristics of all channels.

For the low-energy neutrons a rather good approximation for the S-matrix elements is the single-level Breit-Wigner formula [36B2]

$$S_{ab} = \exp\{-i(\varphi_a+\varphi_b)\}\left(\delta_{ab} - \frac{if_{ra}f_{rb}}{E-E_r-\Delta_r+i\Gamma_r/2}\right) \quad , \qquad (1.5)$$

where E_r is the resonance energy of a excited compound nucleus, Δ_r is the energy shift due to decay channels, φ_a is the potential-scattering phase and f_{ra} is the partial width amplitude connected with the corresponding partial widths Γ_{ra} and the total widths Γ_r of resonances by the relations

$$\Gamma_{ra} = f_{ra}^2, \qquad \Gamma_r = \sum_a \Gamma_{ra} \qquad (1.6)$$

The resonance dependence of the scattering matrix proceeds from a very general physical consideration of the energy distribution for quasi-stationary states of a quantum system [52B2, 58L]. The amplitudes f_{ra} and phases φ_a are real numbers for the isolated resonances. The total width Γ_r in this case defines the lifetime of a corresponding quasi-stationary state $\tau_r = \hbar/\Gamma_r$. So, from an analysis of the resonance structure of neutron cross sections we obtain direct information on the lifetime of a compound nucleus.

Substituting (1.5) into (1.1) one gets the well-known Breit-Wigner formula for the reaction cross section

$$\sigma_{ab} = \pi\lambda\!\!\!^{-2}_a g_a \frac{\Gamma_{ra}\Gamma_{rb}}{(E_r-E)^2+\Gamma_r^2/4} \quad , \qquad (1.7)$$

where the energy shift is included into the corresponding resonance energy. In the same approach the elastic scattering cross section can be written as

$$\sigma_s = \pi\lambda\!\!\!^{-2}_a g_a \left\{4\sin^2\varphi_a + \frac{\Gamma_{ra}[\Gamma_{ra}-2(E_r-E)\sin 2\varphi_a - \Gamma(1-\cos 2\varphi_a)]}{(E_r-E)^2+\Gamma_r^2/4}\right\} \quad . \qquad (1.8)$$

For the elastic scattering the resonance peak is overlaid on the slowly changing background of the potential scattering, and the interference of the potential and resonance scattering distorts the resonance shape. Applying the Breit-Wigner formulae we should bear in mind that both the partial widths and resonance shifts are energy dependent in a common case. These dependencies are not important, as a rule, near resonance energies but they must be taken into consideration at energies far from a resonance.

It is convenient for many applications to write the resonance widths as

$$\Gamma_{rn} = \Gamma_{rn}^{(l)}\sqrt{E}P_l(E) \quad , \qquad (1.9)$$

where the last multiplier describes the penetrability of the centrifugal barrier, which prevents the neutron to escape from a nucleus, and $\Gamma_{ra}^{(l)}$ is called the reduced neutron width. The energy dependence of the centrifugal barrier penetrability P_l, the potential scattering phase φ_l and the level shift Δ_l are usually calculated for the neutron scattering on an impenetrable sphere [52B2, 58L]. For the lowest values of an orbital angular momentum these functions are given in Table 1. As a rule, in calculations of the penetrability the "standard" estimation is used for the nuclear radius: R = (1.23 $A^{1/3}$ + 0.8) fm. This convention is not extended, however, on the radius definition for the potential scattering phases which is usually chosen from an analysis of experimental data or from

calculations of the potential scattering of neutrons within the framework of the optical model (see below). As a result, the effective scattering radius R_s can differ substantially from the value of R and can vary for different orbital momenta.

Table 1. Centrifugal barrier penetrability P_l , potential scattering phase φ_l and level shift Δ_l for an impenetrable sphere with radius R*)

l	P_l	φ_l	Δ_l
0	1	ρ	0
1	$\frac{\rho^2}{1+\rho^2}$	ρ - arctg ρ	$\frac{1}{1+\rho^2}$
2	$\frac{\rho^4}{9+3\rho^2+\rho^4}$	ρ - arctg $\left(\frac{3\rho}{3-\rho^2}\right)$	$\frac{3\left(6+\rho^2\right)}{9+3\rho^2+\rho^4}$

*) $\rho = R/\lambda\!\!\!^{-}_n$

At very low energies the cross sections of neutron reactions are determined by neutrons with the orbital momentum equal to zero (so-called the *s*-wave neutrons). As the neutron widths are proportional to $\sqrt{E}$ and the wave length $\lambda\!\!\!^{-}_n$ is conversely proportional to $\sqrt{E}$, then for $E_i \ll E_r$ Eq. (1.7) can be transformed to

$$\sigma_{nx} = \pi\lambda\!\!\!^{-2}_r \sqrt{\frac{E_r}{E}} \frac{\Gamma_m(E=E_r)\Gamma_{rx}}{E_r^2} \quad . \tag{1.10}$$

It is evident from this formula that at low energies the neutron reaction cross sections obey the $1/v$ law where v is the neutron velocity. The elastic scattering cross section for low energy neutrons can be written as

$$\sigma_s = 4\pi(R_s)^2 + 4\pi\lambda\!\!\!^{-}_n R_s g_n \frac{\Gamma_r}{E_r} + \pi\lambda\!\!\!^{-2}_n g_n \frac{\Gamma_{rn}^2}{E_r^2} \quad . \tag{1.11}$$

Since $\Gamma_r \ll E_r$ the elastic scattering cross section approaches to the asymptotic limit that is defined by the value of the effective potential scattering radius R_s.

Eqs. (1.5)...(1.11) display the simplest example of the one-level description of neutron reaction cross sections. In reality the observed cross sections are formed by the contribution of many resonances. If the resonance widths are much smaller than the spacing between resonances, the resultant cross section may be presented as a superposition of contributions from all isolated resonances, i.e. as the sum of the resonance terms of Eqs. (1.7) and (1.8).

A description of contributions from many resonances can be improved on the basis of the multi-level Breit-Wigner formula for the *S*-matrix

$$S_{ab} = \exp\{-i(\varphi_a + \varphi_b)\}\left(\delta_{ab} - \sum_r \frac{if_{ra}f_{rb}}{E - E_r - \Delta_r + i\Gamma_r/2}\right) \quad . \tag{1.12}$$

The relations for the elastic scattering and reaction cross sections may be written in this case as

$$\sigma_s = 4\pi\lambda\!\!\!^{-2}_a g_a \{\sin^2\varphi_a + \sum_r \left[\frac{\Gamma_{ra}^2}{\Gamma_r^2}\left(\psi_r \,\mathrm{Re}\, C_{raa} + \chi_r \,\mathrm{Im}\, C_{raa}\right) - \frac{\Gamma_{ra}}{\Gamma_r}\psi_r\right] + \\ + \sum_r \frac{\Gamma_{ra}}{\Gamma_r}\left(\psi_r \cos 2\varphi_a + \chi_r \sin 2\varphi_a\right)\} \quad , \tag{1.13a}$$

$$\sigma_{ab} = 4\pi\lambda\!\!\!^{-2}_{a} g_a \sum_r \frac{\Gamma_{ra}\Gamma_{rb}}{\Gamma_r^2}\left(\psi_r \,\mathrm{Re}\, C_{rab} + \chi_r \,\mathrm{Im}\, C_{rab}\right) \quad , \tag{1.13b}$$

where the following functions are used:

$$\psi_r = \frac{\Gamma_r^2/4}{(E-E_r)^2 + \Gamma_r^2/4}; \; \chi_r = \frac{(E-E_r)\Gamma_r/2}{(E-E_r)^2 + \Gamma_r^2/4} \; ; \tag{1.14}$$

$$C_{rab} = 1 + \sum_{s\neq r}\left(\frac{\Gamma_{sa}\Gamma_{sb}}{\Gamma_{sa}\Gamma_{rb}}\right)^{1/2} \frac{i\Gamma_r}{E_r - E_s + i(\Gamma_r + \Gamma_s)/2} \quad . \tag{1.15}$$

The latter function describes the resonance interference which improves essentially the description of the elastic scattering and of the total neutron cross sections for energies between resonances, where background cross sections are determined by “tails" of many resonances.

Both the one-level and multi-level Breit-Wigner formulas are correct for rather small overlap of resonances only. If resonance widths become comparable with resonance spacing, correlations between partial widths of different resonances arise and they play a dominant role in the origin of interference effects. In such cases more general multi-level formulas should be used for the analysis of neutron cross sections [38K, 47W, 58L]. The fairly complete discussion of such formulas can be found in Refs.[68L, 80M].

In most practical applications of resonance formulas it is necessary to take into consideration the finite resolution of neutron spectrometers and Doppler broadening, caused by the thermal motion of target nuclei. It is usually assumed that the distribution of target nuclei velocities obeys the Maxwell distribution with the effective temperature T_{eff}. The distribution of relative kinetic energies E' of target nuclei may be written as

$$f(E,E')dE' = \frac{1}{\sqrt{\pi}\Delta}\exp\left[-\frac{(E-E')^2}{\Delta^2}\right]dE' \tag{1.16}$$

where $\Delta = 2\,[T_{eff}E/(1.A+1)]^{1/2}$ is called the Doppler width. To take into account some difference between the velocity distribution of target nuclei and the Maxwell distribution of velocities in an ideal gas, the temperature T_{eff} is chosen, as a rule, a little higher than the real temperature of a target. It is common practice to estimate this temperature excess in the framework of the Debye model for the vibrational spectra of target atoms [39L].

Averaging the cross sections in the center of mass system over the distribution (1.16) one gets the following formula for the cross sections in the lab-system

$$\sigma(E) = \int_0^\infty \sigma(E')f(E,E')dE' \quad . \tag{1.17}$$

Using the Breit-Wigner formulas here one obtains the previous relations (1.13), but the following functions should be substituted into them instead of functions (1.14):

$$\psi_r(\beta,x) = \frac{1}{\beta\sqrt{\pi}}\int_{-\infty}^{\infty} dy \exp\left[-\frac{(x-y)^2}{\beta^2}\right](1+y^2)^{-1} \quad ,$$

$$\chi_r(\beta,x) = \frac{1}{\beta\sqrt{\pi}}\int_{-\infty}^{\infty} dy \exp\left[-\frac{(x-y)^2}{\beta^2}\right]y(1+y^2)^{-1} \quad , \tag{1.18}$$

where $x = 2(E\text{-}E_r)/\Gamma_r$ and $\beta = 2\Delta/\Gamma_r$. Functions (1.18) are applied widely not only in nuclear physics, but also in the theory of atomic spectra. These functions can be connected with the probability integral from a complex argument and fast computer codes are available for their calculations [76C]. Analyzing the functions (1.18) it is not difficult to show that the thermal motion of target nuclei results in an additional broadening of resonances. Because integrals from functions $\psi_r(x)$ and $\chi_r(x)$ do not depend on temperature, the area under a resonance curve remains unchanged.

The Doppler broadening plays a relatively small role in the analysis of wide s-wave resonances of light and medium nuclei, but it should be certainly taken into consideration in the description of very narrow *p*- and *d*-wave-resonances of these nuclei. For heavy nuclei the Doppler broadening is important also for most s-wave resonances. The broadening of resonances due to the finite resolution of neutron spectrometers could be described in the same way as the Doppler broadening. The value of Δ in this case is defined by the resolution of a spectrometer.

Nowadays the numerous experimental data on neutron resonance parameters are obtained by efforts of many laboratories. A most complete compilation of available data is given in Refs. [81M, 84M]. A distinctive feature of resonance parameters is strong fluctuations of the neutron resonance widths reflecting a complex structure of excited nuclear states.

For isolated resonances the partial widths are defined as the squares of real amplitudes (1.6) which determine the overlap of the wave function of the compound nucleus with the wave function of residual nucleus and the emitted particle. Due to the complex structure of compound nucleus states the product of their wave functions and channel wave functions oscillates so strongly that the positive and negative contributions almost cancel each other. The overlap integral for such functions will be close to zero, and for various states it can deviate with approximately equal probability both on the positive and on the negative side. It is natural to suppose in these conditions that the distribution of reduced resonance amplitudes should have the gaussian-form

$$P(f_n)df_n = \frac{1}{\sqrt{2\pi\left\langle f_n^2\right\rangle}}\exp\left(-\frac{f_n^2}{2\left\langle f_n^2\right\rangle}\right)df_n \quad , \tag{1.19}$$

where the angular bracket indicates averaging over resonances. Assuming the distribution (1.19) as a hypothesis, Porter and Thomas derived the distribution for the reduced partial widths [56P]

$$P(\Gamma_n)d\Gamma_n = \frac{1}{\sqrt{2\pi\Gamma_n\left\langle\Gamma_n\right\rangle}}\exp\left(-\frac{\Gamma_n}{2\left\langle\Gamma_n\right\rangle}\right)d\Gamma_n \quad . \tag{1.20}$$

In Fig. 1 this distribution is shown in comparison with experimental data on neutron widths of *s*-wave resonances observed in the ^{238}U + n reaction. Similar results currently are available for many nuclei [72C, 72L].

The Porter-Thomas distribution assumes that partial widths relate to the same decay channel. If several channels contribute to observed resonance widths, then their distribution should be found as a convolution over distributions of partial widths. If the average partial widths for ν independent channels are equal, then the distribution for the corresponding total widths will be described by the χ_ν^2 - distribution for ν degrees of freedom

$$P_\nu(\Gamma)d\Gamma = \left[\frac{\nu\Gamma}{2\left\langle\Gamma\right\rangle}\right]^{\nu/2}\frac{\exp\left[-\nu/2\left\langle\Gamma\right\rangle\right]}{\left(\frac{\nu}{2}-1\right)!\,\Gamma}d\Gamma \quad . \tag{1.21}$$

The fluctuation of widths corresponding to this distribution may be characterized by the width dispersion

$$\left\langle\left(\Gamma-\left\langle\Gamma\right\rangle\right)^2\right\rangle = \frac{2}{\nu}\left\langle\Gamma\right\rangle^2 \quad . \tag{1.22}$$

It is evident that the dispersion is maximal for the single-channel distribution (1.20) and decreases with the growth of the number of decay channels.

Together with the width distribution significant interest is evoked by the statistical regularities of the spacings between resonances. The basic problem in a description of spacing distributions is the account of a residual interaction responsible for the well-known effect of the level repulsion. Analyzing this repulsion on the basis of a rather simple model, Wigner obtained the nearest-neighbour spacing distribution for levels with a given spin and parity [51W1]

$$P(E)dE = \frac{\pi E}{2D^2}\exp\left(-\frac{\pi E^2}{4D^2}\right)dE \quad , \tag{1.23}$$

where D is the mean level spacing.

To study the statistical consequences of the level repulsion more deeply, Wigner suggested to consider the Hamiltonian of the system as random matrices [51W1]. The main idea of such an approach is the replacement of matrix elements of a complex residual interaction of physical systems by the random variables with a simple statistical distribution. At first the so-called Gaussian orthogonal ensemble was investigated [65P] which consists of real symmetric matrices with statistically independent elements and has the distribution of eigen values invariant relative to a rotation in Hilbert space. For such an ensemble with the matrices of 2×2 dimension the spacing distribution of two eigen values coincides with the distribution (23). For the matrices of higher dimensions some difference of distributions arises but it is rather small.

The problem of the level spacing distribution was put on a more rigorous formal basis by Dyson [62D]. He exposed the hypothesis of statistical independence of matrix elements to criticism and introduced the circular orthogonal ensemble, which permits to study the eigen values distribution for random matrices without consideration of the level density energy dependence. Using the analogy with electrostatics Dyson demonstrated the physical sense of level repulsion, specified the level spacing distribution for large spacings, and explored high order correlations in the level distributions.

To reconcile the statistical properties of levels with the shell model conceptions, the two-body random ensembles were explored [75B2, 81B]. The configuration spaces in such approaches are constructed on the basis of the realistic level schemes of the shell-model and only the matrix elements of residual two-body interaction are regarded as random variables. This statistical extension of the shell model seems much more physical than the orthogonal ensemble model, but the spacing distributions obtained for both models are very similar.

In the past years the spectral distributions of neutron resonances have been analyzed by many authors [65P, 72C, 81B]. As an example the spacing distribution between the nearest s-wave resonances observed in the reaction ^{238}U + n is shown in Fig. 2. The analysis of such distributions requires a reliable identification of resonances to separate weak s-wave resonances from numerous p-wave resonances. For high quality experimental data the resonance spacing distributions agree quite well with the predictions of the random ensemble models.

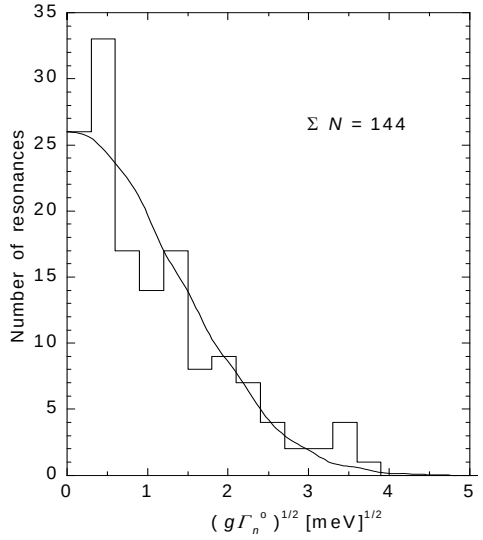

Fig. 1. Distribution of the reduced neutron widths for s-wave resonances in the reaction ^{238}U + n (histogram), the solid curve corresponds to the Porter-Thomas distribution.

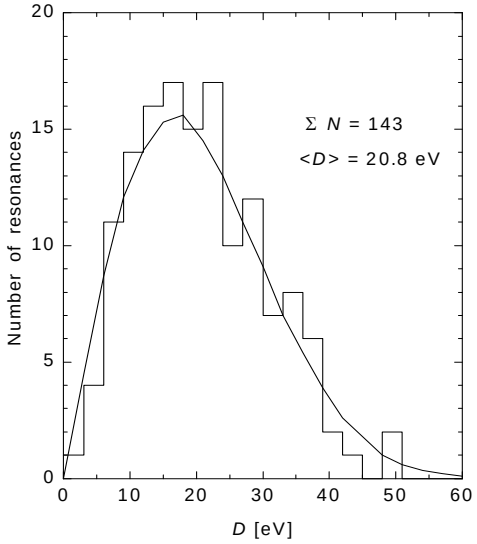

Fig. 2. Nearest-neighbour spacing distribution for s-wave resonances in the reaction ^{238}U + n (histogram), the solid curve corresponds to the Wigner distribution.

Only a brief consideration of some most important applications of the random ensemble theory was given above. The study of such ensembles created in fact a new direction of statistical research with its own specific methods and problems. More complete discussions of these problems as well as many applications of the theory may be found in monographs [67M1, 68L, 81B].

2 Statistical description of average neutron cross sections

With an increase in the neutron energy the widths of resonances grow and the resonance spacings decrease. As a result the resonances begin to overlap and observed cross sections are determined by the contribution of many resonances. A similar result is obtained for neutron spectrometers with a bad resolution, when measured cross sections are formed by the cumulative effect of many isolated resonances. The methods of description of such cross sections may be considered using the example of reactions induced by s-wave neutrons.

Let us average the matrix elements (1.12) over the energy interval ΔE that includes a large number of resonances

$$\overline{S}_{ab} = \frac{1}{\Delta E}\int_{E-\Delta E/2}^{E+\Delta E/2} S_{ab}(E)dE = \exp\left[-i(\varphi_a+\varphi_b)\right]\left(\delta_{ab} - \frac{\pi}{D}\langle f_a f_b\rangle\right) , \tag{2.1}$$

where we use a bar to indicate an energy average and angular brackets to indicate an average over many resonances. It is assumed implicitly in this expression that the phases of potential scattering and average resonance parameters do not change on the interval considered. If the amplitudes of resonances fluctuate in a random way, then for $a \neq b$ we may expect $\langle f_a f_b\rangle = 0$ and the averaged S-matrix has to be diagonal

$$\overline{S}_{ab} = \delta_{ab}\exp(-2i\varphi_a)\left(1 - \frac{\pi}{D}\langle\Gamma_a\rangle\right) . \tag{2.2}$$

With a similar averaging of the squares of matrix elements we find:

$$\begin{aligned} \overline{|S_{aa}|^2} &= 1 - \frac{2\pi}{D}\langle\Gamma_a\rangle + \frac{2\pi}{D}\left\langle\frac{\Gamma_a^2}{\Gamma}\right\rangle , \\ \overline{|S_{ab}|^2} &= \frac{2\pi}{D}\left\langle\frac{\Gamma_a\Gamma_b}{\Gamma}\right\rangle \text{ for } a \neq b . \end{aligned} \tag{2.3}$$

On the basis of these formulae the average cross sections of the elastic scattering, the reactions and the total interaction can be expressed as

$$\begin{aligned} \overline{\sigma}_s &= \pi\lambda\!\!\!^{-2}_a\overline{|1-S_{aa}|^2} = \sigma_s^{opt} + \sigma_s^{fluct} , \\ \overline{\sigma}_r &= \sum_{a\neq b}\sigma_{ab} = \sigma_r^{fluct} , \\ \overline{\sigma}_t &= 2\pi\lambda\!\!\!^{-2}_a\left(1 - \mathrm{Re}\,\overline{S}_{aa}\right) . \end{aligned} \tag{2.4}$$

In accordance with the definition given by Feshbach, Porter and Weiskopf [54F] we will refer to the cross sections expressed through the averaged elements of S-matrix as the optical ones and the cross sections determined by the dispersion of matrix elements as the fluctuating ones:

$$\begin{aligned} &\sigma_s^{opt} = \pi\lambda\!\!\!^{-2}_a\left|1-\overline{S_{aa}}\right|^2 ; \qquad \sigma_{ab}^{fluct} = \frac{2\pi^2\lambda\!\!\!^{-2}_a}{D}\left\langle\frac{\Gamma_a\Gamma_b}{\Gamma}\right\rangle ; \\ &\sigma_s^{fluct} = \pi\lambda\!\!\!^{-2}_a\left(\overline{|S_{aa}|^2} - \left|\overline{S}_{aa}\right|^2\right) = \pi\lambda\!\!\!^{-2}_a\left(\frac{2\pi}{D}\left\langle\frac{\Gamma_a^2}{\Gamma}\right\rangle - \frac{\pi^2}{D^2}\langle\Gamma_a^2\rangle\right). \end{aligned} \tag{2.5}$$

It was shown in the framework of the time dependent scattering theory that the optical cross sections define the probability of elastic or inelastic scattering of a particle wave package during its transmission through a nucleus, whereas the fluctuating cross sections define the probability of particle emission delayed by the lifetime of a compound nucleus [55F]. So σ_s^{opt} determines the cross

section of the direct elastic scattering of a particle on a nuclear potential, while σ_s^{fluc} determines the cross section of the elastic scattering through the intermediate stage of a compound nucleus.

The cross section of compound nucleus formation may be written with the help of Eqs. (2.4) and (2.5) in the form of

$$\sigma_c = \sigma_s^{fluct} + \sigma_r^{fluct} = \pi\lambda\!\!\!^{-2}_a T_a \quad , \tag{2.6}$$

where the transmission coefficient T_a is defined as

$$T_a = 1 - \left|\overline{S}_{aa}\right|^2 = \frac{2\pi}{D}\langle\Gamma_a\rangle - \frac{\pi^2}{D^2}\langle\Gamma_a\rangle^2 \tag{2.7}$$

The diagonal elements of the average scattering matrix are usually approximated by means of the optical model [54F]. Some basic components of the optical model and its application to an experimental data analysis will be considered below.

The average reaction cross section may be written in the form of

$$\overline{\sigma}_{ab}^{fluct} = \frac{2\pi^2\lambda\!\!\!^{-2}_a}{D}\frac{\langle\Gamma_a\rangle\langle\Gamma_b\rangle}{\sum_c\langle\Gamma_c\rangle}F_{ab} \quad , \tag{2.8}$$

where $F_{àb}$ is the width fluctuation correction that determines the difference between the averaged ratio of fluctuating widths and the ratio of the average widths:

$$F_{ab} = \left\langle \frac{\Gamma_a\Gamma_b}{\sum_c\Gamma_c} \right\rangle \Bigg/ \frac{\langle\Gamma_a\rangle\langle\Gamma_b\rangle}{\sum_c\langle\Gamma_c\rangle} \quad . \tag{2.9}$$

If the second term in the transmission coefficient estimation (2.7) can be neglected, Eq. (2.9) may be written in the form of

$$\overline{\sigma}_{ab}^{fluct} = \pi\lambda\!\!\!^{-2}_a \frac{T_a T_b}{\sum_c T_c} F_{ab} \quad . \tag{2.10}$$

This expression is usually called the Hauser-Feshbach formula that was primarily derived without the width fluctuation correction [51W2, 52H].

An explicit relation for the width fluctuation correction (2.9) can be found rather simply if the distributions of fluctuating widths are known. Applying the Porter-Thomas distribution to the neutron widths of resonances and assuming that the radiative widths do not fluctuate, one can obtain the fluctuation corrections for the elastic and inelastic neutron scattering [64M]

$$F_{ab} = (1+2\delta_{ab})\sum_c T_c \int_0^\infty \frac{\exp(-tT_\gamma)dt}{(1+2tT_a)(1+2tT_b)\prod_{c\neq\gamma}(1+2tT_c)^{1/2}} \quad . \tag{2.11}$$

The correction for the radiative neutron capture has the form

$$F_{a\gamma} = \sum_c T_c \int_0^\infty \frac{\exp(-tT_\gamma)dt}{(1+2tT_a)\prod_{c\neq\gamma}(1+2tT_c)^{1/2}} \quad , \tag{2.12}$$

where the transmission coefficient for the radiative capture is defined as $T_\gamma = 2\pi\Gamma_\gamma/D$. The sums in Eqs. (2.11) and (2.12) include all competing channels of a compound nucleus decay, while the products in the denominators of (2.11) and (2.12) include all channels except the radiative one.

The width fluctuation correction increases the compound elastic scattering cross section and reduces the inelastic scattering cross sections. Taking into account such corrections is essential for a small number of open channels. For example, the fluctuation corrections reduce the neutron inelastic scattering cross sections on the low-lying levels at near threshold energies by almost 50% as compared with the simple Hauser-Feshbach formula [64M]. The effect of fluctuation corrections on inelastic scattering cross sections decreases with the growth of the number of open channels, while the correction for the compound elastic scattering cross section increases and it can reache an almost maximum value of 3.

With the increase in energy the resonances begin to overlap and interference effects start to play an increasingly important role. As before, we are interested in the description of cross-sections averaged over the energy interval containing many resonances. In the region of isolated resonances the average cross sections were formed as a sum of independent contributions from each of the excited states of a compound nucleus. By contrast to this, in the case of strong resonance overlapping many excited states lying within the resonance width interval take part in the reaction and this fact introduces new aspects into the description of average reaction cross sections.

The general expression for the elements of the scattering matrix in the overlapping resonance range can be written in the following form

$$S_{ab} = S_{ab}^{opt} - i\sum_r \frac{g_{ra} g_{rb}}{E - E_r + i\,\Gamma_r/2} \quad , \tag{2.13}$$

where, unlike the isolated resonance case, the channel resonance amplitudes g_{ra} may be complex, while $S_{ab}{}^{opt}$ values determine the non-diagonal elements of the scattering matrix which are weakly dependent on energy . The averaged elements of the S -matrix, as well as the average reaction cross sections can be found in a way similar to Eqs. (2.2)-(2.5). However, in these calculations we should take into account the correlation of amplitudes for overlapping resonances, the important role of which was shown in Refs. [67M2, 74W, 74T, 75M].

Let us consider the relation of the resonance parameters and the elements of the averaged S-matrix for the case $S_{ab}{}^{opt} = 0$. Proceeding from the unitary condition (3) we can obtain a certain "sum rule" for the resonance amplitudes

$$\frac{2\pi}{D}\left\langle g_a^2 \right\rangle = \overline{S}_{aa}^{*-1} - \overline{S}_{aa} \quad . \tag{2.14}$$

As the diagonal elements of the averaged S-matrix are described by the optical model, we can use the definition of the transmission coefficients (2.7) and rewrite (2.14) in the form

$$\frac{2\pi}{D}\left\langle g_a^2 \right\rangle = T_a \Big/ \sqrt{1 - T_a} \quad . \tag{2.15}$$

On the other hand, we can obtain the connection between the transmission coefficients and partial resonance widths

$$T_a = 1 - \exp\left(-\frac{2\pi\langle \Gamma_a \rangle}{D} \right) \; ; \; \langle \Gamma \rangle = \sum_a \Gamma_a \quad . \tag{2.16}$$

The latter equation for the average resonance width can also be written as

$$\frac{2\pi}{D}\langle \Gamma \rangle = \sum_a \ln\left(1 - T_a\right)^{-1} \quad . \tag{2.17}$$

The above formulas show that when T_a approaches unity, the average partial and total widths tend to infinity, while the absolute values of amplitudes squared grow exponentially as compared to partial widths [67M2].

Let us return to the analysis of the average cross sections. For fluctuating cross sections in the overlapping resonance range we get

$$\sigma_{ab}^{fluct} = \pi\lambda\!\!\!^{-2}_a \left\{ \frac{2\pi}{D} \left\langle \frac{|g_a|^2 |g_b|^2}{\Gamma} \right\rangle - M_{ab} \right\} \quad , \tag{2.18}$$

where

$$M_{ab} = 2\left|\overline{S}_{ab} - S_{ab}^{opt}\right|^2 - \frac{2\pi i}{D} \left\langle \sum_{s \neq r} \frac{g_{ra} g_{rb} g_{sa}^* g_{sb}^*}{E_r - E_s + i\left(\Gamma_r + \Gamma_s\right)/2} \right\rangle \quad . \tag{2.19}$$

The first term of (2.18) is similar to the Hauser-Feshbach formula, however, its notation through the transmission coefficients depends to a large extent on the correlation properties of the resonance amplitudes g_{ra} . These properties are not well known. Nevertheless, we can assume that $|g_{ra}|^2$ values are proportional to the partial widths Γ_{ra} and the proportion coefficient is independent of the channel index

$$\left|g_{ra}\right|^2 \Big/ \Gamma_{ra} = N_r >> 1 \quad . \tag{2.20}$$

Based on this assumption Moldauer [67M2] introduced the effective transmission coefficients

$$\Theta_{ra} = \frac{2\pi}{D} N_r \left|g_{ra}\right|^2 \ , \ \Theta_r = \sum_a \Theta_{ra} \quad , \tag{2.21}$$

which are related to the optical transmission coefficients through the following equations

$$T_a = 1 - \sum_{b \neq a} \left|S_{ab}^{fluct}\right|^2 = \left\langle \Theta_a \right\rangle - \sum_{b \neq a} M_{ab} \quad , \tag{2.22}$$

and with the help of which the reaction cross section (2.18) can be written in the form

$$\sigma_{ab}^{fluct} = \pi \lambda\!\!\!^{-2}_a \left(\left\langle \frac{\Theta_a \Theta_b}{\sum_c \Theta_c} \right\rangle - M_{ab} \right) \quad . \tag{2.23}$$

If the coefficients θ_a are expressed via optical transmission coefficients, in the general case we get a rather complicated formula for the fluctuating cross sections. However, for the overlapping resonances the correlations of θ_{ra} values seem to be very significant for different channels [74W, 74T, 75M]. These correlations could lead to an effective cancellation of terms with different M_{ab} and, thus, to a certain simplification of the description of average cross sections. If we assume that such "*M*-cancellation" is a common property of the overlapping resonances, we obtain the former Hauser-Feshbach formula for the reaction cross section with a correction factor for width fluctuations (2.10). However, this correction factor should be defined in view of the difference between the overlapping resonance widths distribution and a similar distribution in the isolated resonance range. The growth of Γ_a/D is expected to bring an increase in the effective number of the degrees of freedom ν for partial widths from 1 to the limiting value of 2. The distribution of widths in this case will be described by the corresponding χ_ν^2 - distribution. Using (1.21), we obtain the following equation for the width fluctuation correction in the elastic and inelastic scattering channels

$$F_{ab} = \left(1 + \frac{2}{\nu_a}\delta_{ab}\right) \sum_c T_c \int_0^\infty \frac{\exp\left(-tT_\gamma\right) dt}{\left(1 + \frac{2t}{\nu_a} T_a\right)\left(1 + \frac{2t}{\nu_b} T_b\right) \prod_{c \neq \gamma} \left(1 + \frac{2t}{\nu_c} T_c\right)^{\nu_c/2}} \quad . \tag{2.24}$$

Similar changes will be introduced in the width fluctuation correction (2.12) for the radiative neutron capture. An increase in ν leads to a certain decrease in the influence of width fluctuation corrections. In particular, a maximum increase in the elastic scattering cross section through a compound nucleus for $\nu_a = 2$ will reach a factor 2 only, while in the isolated resonance range this increase would reach 3.

A rather simple approximation to the Hauser-Feshbach formula was proposed in Ref. [74T]. Instead of introducing the correction factor the authors suggested to use the modified transmission coefficients determined as

$$\Im_a = T_a \Big/ \left(1 + \frac{2}{\nu_a} \frac{T_a}{\sum_c T_c}\right) \quad . \tag{2.25}$$

It was proved by the statistical modeling of the average cross sections that this approximation is good enough when the total number of open reaction channels is not small [74T, 75M]. In Ref. [75H] more precise though more complex definitions of the modified transmission coefficients were discussed. An empirical formula for the effective number of channels based on a computational modeling of average cross sections in the region of overlapping resonances was found

$$\nu_a = 1 + T_a^{1/2} \quad . \tag{2.26}$$

Though the formula is not very precise, it nevertheless reflects the general trends of changes of width fluctuation effects for the overlapping resonances.

The above analysis is based on the assumption about the diagonal form of the *S*-matrix, that is equivalent to the assumption about the absence of any direct nuclear reactions for inelastic channels. Non-resonance non-diagonal elements of the *S*-matrix correspond to direct transitions, an introduction of which should lead to additional correlations between the partial widths of different decay channels of a compound nucleus. These correlations, in turn, can lead to an increase in the fluctuating component of the average reaction cross sections. The nature of this effect is the same as the increase of the elastic scattering cross section through a compound nucleus due to width fluctuations. The general methods of the analysis of the fluctuating cross sections taking account of direct processes were developed in Refs. [74W, 75M]. It was proved that in this case the average cross sections of the reaction through a compound nucleus can be written in the form of the Hauser-Feshbach formula with the modified width fluctuation corrections and transmission coefficient determined with an allowance for direct transitions. With direct processes included the intensity of the fluctuating component of cross sections grows due to partial width correlations in the channels linked by direct transitions only when the number of open channels is rather small. As the number of open channels increases, the correlation effects weaken and simple superpositions of the cross sections of direct reactions and reactions through a compound nucleus take place.

For a relatively large number of channels the sum of the transmission coefficients in the numerator and denominator of the Hauser-Feshbach formula (2.10) should be replaced by integrals

$$\sum_c T_c = \sum_{l,j,I} \int_0^{U_{\max}} T_{lj}(E_c)\rho(U,I)dU \quad , \qquad (2.27)$$

which contain the level densities of residual nuclei. The sum in (2.27) is taken over all combinations of the angular momenta and spins of the reaction products possible for given quantum characteristics of the compound nucleus. With an increase in the number of channels the level density plays an increasingly important role in the correct description of reaction cross sections passing through the compound nucleus stage.

Initially the compound nucleus model formulated by N.Bohr [36B1] was considered as a model of strong interaction of the projectile with the target nucleus. As a result of such an interaction the projectile is absorbed by the target nucleus immediately at the moment of contact and the compound nucleus formation cross section should coincide with the geometric cross section of the nucleus. Further research demonstrated however that for most reactions absorption is not so strong and the nucleus should be considered rather as a “semi-transparent” body.

Indications of the significant transparency of nuclei were first obtained from the analysis of the neutron scattering cross sections with the energy of 90 MeV [49F]. In order to describe the observed total and absorption cross sections a complex single-particle potential was used. Its real part corresponds to the mean field of a nucleus while the imaginary part determines the overall effect of all inelastic processes that remove the particle from the elastic channel. The relation between the imaginary part of the potential and the nuclear absorption coefficient was obtained from the consideration of the particle flux attenuation.

A further developments of the optical model was stimulated by the experiments on the scattering of neutrons with energies of several MeV conducted by Barshall [52B1]. Wide maxima were observed in the energy dependence of the neutron total cross sections, the positions of which changed smoothly with the mass number. Later similar maxima were observed in the differential neutron scattering cross sections as well. Feshbach, Porter and Weiskopf [54F] demonstrated that common features of the observed cross sections can be reproduced within the optical model with the potential in the form of a complex square-well with the depth of 42(1 + 0.03i) MeV and radius $R_o = 1.45\ A^{1/3}$ fm. The imaginary potential value corresponds to the mean free path of 15-20 fm, which significantly exceeds the size of a nucleus. Thus nuclei are rather transparent for low-energy particles and this property plays an important role in the analysis of nuclear reactions.

Though the square well model describes the basic features of the irregular behavior of the strength functions and the corresponding scattering cross sections, it is certainly too simplified to quantitatively describe experimental data. Therefore further development of the optical model

proceeded by making the single-particle potential used more precise and complicated. At present this potential usually takes the form

$$V(r) = -(V_v + iW_v) f_v(r) + 4iW_s a_s \frac{df_s}{dr} + V_{so} \frac{\lambda\!\!\!^{-2}_{\pi}}{r} \frac{df_{so}}{dr} (\mathbf{l} \cdot \mathbf{s}) \quad , \qquad (2.28)$$

where $f_i(r) = [1 + \exp(\frac{r - R_i}{a_i})]^{-1}$ are the form-factors of the volume, surface and spin-orbital components of the optical potential, respectively, and the geometric parameters of the corresponding form-factors can be different in the general case. Numerous results of cross section calculations within the optical model as well as examples of the experimental data description obtained can be found in Refs. [60N, 63H].

Many authors attempted to find a universal set of optical potential parameters, which would give rather good description of a wide range of experimental data. At the same time they tried to keep the same geometrical parameters of the potential as in the shell model. They also take into consideration the dependence of the real and imaginary optical potential components on both the projectile energy and target isospin [72P1, 73H]. Despite the large number of the parameters included in the analysis, calculations with universal sets of potential parameters reproduce correctly only the general trends of the cross section dependencies on the energy and nuclear mass number. To describe the cross sections in a particular nucleus a certain adjustment of the potential parameters is usually needed, especially when cross sections are related to the low-energy region. The strength functions of the *s*- and *p*-wave neutrons shown in Fig. 3 can serve as an example of the results obtained within the optical model calculations. The calculations performed for some universal set of optical potential parameters do not reproduce the isotopic changes of the strength functions observed in the range of strength function minima. Neither does it show the splitting of *s*-wave strength functions in the rare-earth nuclei. For a more accurate description of the available data we should not limit ourselves to the one-channel optical model and include some additional structural effects.

In the one-channel model the influence of all possible reaction channels on the elastic scattering channel is approximated by means of the imaginary part of the optical potential. If the effect of some reaction channels is much stronger than that of others, as we observe, for example, for the inelastic scattering of nucleons on the low-lying collective levels, the generalized optical model or the of coupled channels method (CCM) [58F1, 65T] should be used instead of the one-channel model. Within the phenomenological version of CCM the interaction between the neutron and the nucleus is described by the deformed optical potential

$$V(\mathrm{r}) = V(r) + V_{coupl}(r, \theta, \varphi) \quad , \qquad (2.29)$$

where *V(r)* is the spherical part of the potential similar to (2.28) and V_{couple} is the potential component responsible for the coupling of different reaction channels. V_{couple} can be expressed through the deformation parameters that describe the rotational or vibrational nuclear excitations [65T]. The coupling of the elastic scattering channel and those of closed inelastic scattering channels corresponding to low- lying collective levels is directly responsible for the splitting of the 3s-giant resonance of the neutron strength functions shown in Fig. 3 [57M, 58V, 58C]. The coupling with the inelastic scattering channels is also important for the explanation of the isotopic dependence of the neutron strength functions [72N].

Nowadays CCM is extensively used in the neutron cross-section analysis and numerous examples of experimental data descriptions obtained can be found in Refs. [75T, 83B]. The optical potential parameters obtained on the basis of the CCM analysis demonstrate a much smaller fluctuation from nucleus to nucleus than the individual sets of spherical optical model parameters. Besides, the parameters of the real component of the optical potentials are also in a much better agreement with the standard parameters of the shell model single-particle potential. This agreement is an important advantage of the generalized optical model.

When the mean free path is long, the probability of one of the particles escaping from the nucleus after one or several collisions of the projectile with a nucleon of the target nucleus is rather

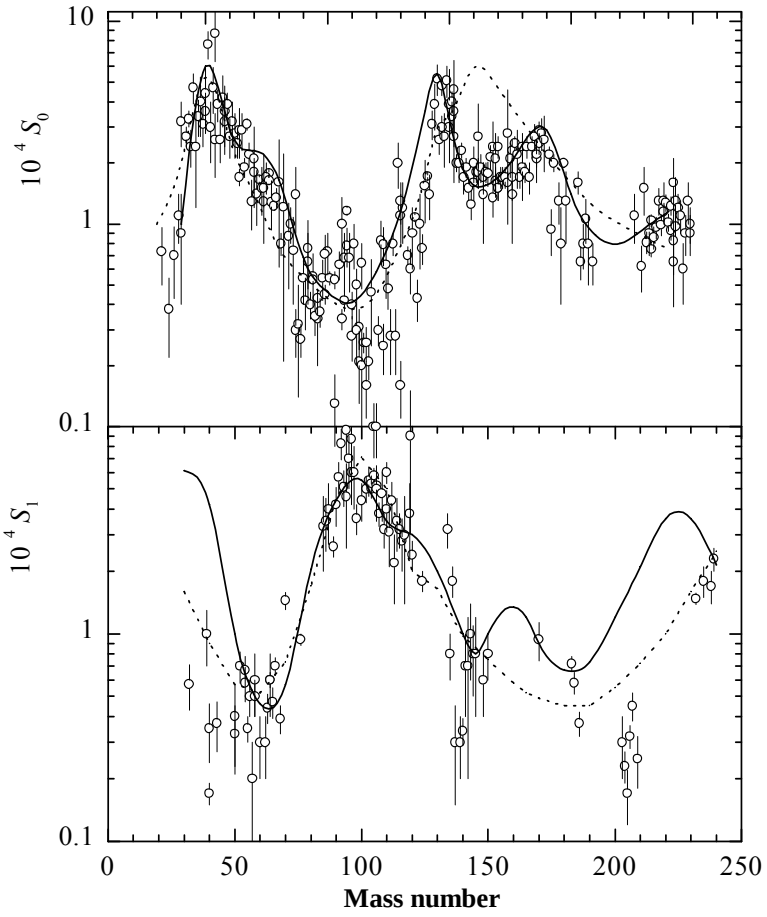

Fig. 3. Strength functions of s- and p-wave neutrons as a function of the mass number. Results of calculations are shown by dashed curves for the spherical optical model and solid ones for CCM.

high. Such processes are usually referred to as direct nuclear reactions. A typical time of direct reactions is approximately the same as the transit time of a projectile ~10^{-22} s and is much shorter than the time-life of a compound nucleus $\tau_c = 10^{-1}..10^{-19}$ s. As the number of intranuclear collisions is small, they cannot sufficiently disorient the projectile, thus the particle escaping from the nucleus is usually concentrated in the front hemisphere. This asymmetrical character of the angular distribution of particles is a major characteristic of direct mechanisms of nuclear reactions. The main theoretical methods used nowadays to describe these reactions as well as numerous examples of their application in experimental data analysis can be found in Refs. [70A, 83S].

The above time estimates show that direct transitions and comparatively slow processes in the stage of the quasi-equilibrium compound nucleus correspond to two extremes in the time scale of nuclear reaction evolution. It is natural to expect that the processes relevant to the intermediate transition stage between the fast direct and slow compound stages will play a certain part in the nuclear transformations too. Study of such processes is one of the major current concerns in the theory of nuclear reactions [74F, 75A, 80F].

3 Nuclear level densities

An essential part of our current knowledge on nuclear structure has obtained from investigations of the low-lying nuclear levels. However, a number of levels for medium and heavy nuclei grow so rapidly with increasing excitation energy that the spectroscopic analysis for each level becomes practically unfeasible. In such conditions a transition to the statistical description of nuclear properties looks natural and quite reasonable. The nuclear level density is the most important statistical characteristics of excited nuclei.

Simple analytical relations for the state density $\omega(U)$ of a nucleus with a given excitation energy U and the level density $\rho(U,J)$ of a nucleus with a given angular momentum J have been obtained by Bethe on the basis of the Fermi gas model [37B]:

$$\omega(U) = \frac{\sqrt{\pi}}{12a^{1/4}U^{5/4}} \exp\left(2\sqrt{aU}\right)$$
$$\rho(U,J) = \frac{2J+1}{2\sqrt{2\pi}\sigma^3}\,\omega(U)\exp\left[-\frac{(J+1/2)^2}{2\sigma^2}\right] \qquad (3.1)$$

Here $a = \pi^2 g/6$ is the level density parameter, which is proportional to the single-particle state density g near the Fermi energy, and σ^2 is the spin cutoff parameter.

For the Fermi gas model the state equations determining a dependence of the excitation energy U, the entropy S and other thermodynamic functions of a nucleus on its temperature t have a simple form:

$$U = at^2 \quad , \qquad S = 2at \quad , \qquad \sigma^2 = \langle m^2 \rangle gt \quad , \tag{3.2}$$

where $\langle m^2 \rangle$ is the mean square value of the angular momentum projections for the single-particle states around the Fermi energy, which may also be associated with the moment of inertia of a heated nucleus $\Im = g\langle m^2 \rangle$. The connection of the thermodynamic functions (3.2) with the state and level densities (3.1) is obvious.

The main parameters of the Fermi-gas model may be estimated rather simply using the semiclassical approximation:

$$a = 2\left(\frac{\pi}{3}\right)^{4/3} \frac{m_o r_o^2}{\hbar^2} A\left(1 + b_s A^{-1/3}\right), \qquad \Im_0 = \frac{2}{5}\frac{m_0 r_0^2}{\hbar^2} A^{5/3} \tag{3.3}$$

where m_0 is the nucleon mass, r_0 is the radial parameter, A is the mass number and b_s defines the surface component of the single-particle level density.

The most direct information on the level density of highly excited nuclei is obtained from the average parameters of neutron resonances. For the majority of nuclei the observed resonances correspond to s-neutrons, therefore the value of D_0 is related to the level density of the compound nucleus by the relations:

$$D_0^{-1} = \begin{cases} \frac{1}{2}\left\{\rho(B_n + \Delta E/2, I_0 + 1/2) + \rho(B_n + \Delta E/2, I_0 - 1/2)\right\} & for\ I_0 \neq 0 \quad , \\ \frac{1}{2}\rho(B_n + \Delta E/2, 1/2) \quad for\ I_0 = 0 \quad , \end{cases} \tag{3.4}$$

were B_n is the neutron binding energy, ΔE is the energy interval for which the resonances are being examined, I_0 is the target nucleus spin, and the coefficient 1/2 before the sum takes into account the fact that s-neutrons form resonances only of a particular parity. If necessary, resonances for p-neutrons can be taken into consideration analogously.

The experimental values of D_s are normally used as source data, from which the magnitude of the level density parameter can be derived by means of Eqs. (3.1) and (3.4). Many authors have carried out such an analysis [65G, 69M, 70B]. The regular differences of the level densities for even-even, odd and even-odd nuclei analogous to the even-odd differences of the nuclear masses have been already noted on the first systematics of experimental data. To take this effect into account it is usual to introduce the so-called effective excitation energy defined as

$$U^* = U - \begin{cases} \delta_Z + \delta_N \text{ for even - even} \\ \delta_Z \text{ for even Z} \\ \delta_N \text{ for even N} \\ 0 \text{ for odd - odd} \end{cases} \tag{3.5}$$

where δ_I is the corresponding phenomenological correction for even-odd differences of the nuclear binding energies.

The level density parameters obtained in the framework of such an approach are shown in the upper part of Fig. 4. The values of a -parameters differ greatly from the semi-classical estimation (3.3). In the lower part of Fig. 4 the shell corrections to the nuclear mass formula are shown which are determined as

$$\delta E_0 = M_{\exp}(Z, A) - M_{ld}(Z, A, \beta) \quad , \tag{3.6}$$

where M_{exp} is the experimental value of the mass defect and M_{ld} is the liquid drop component of the

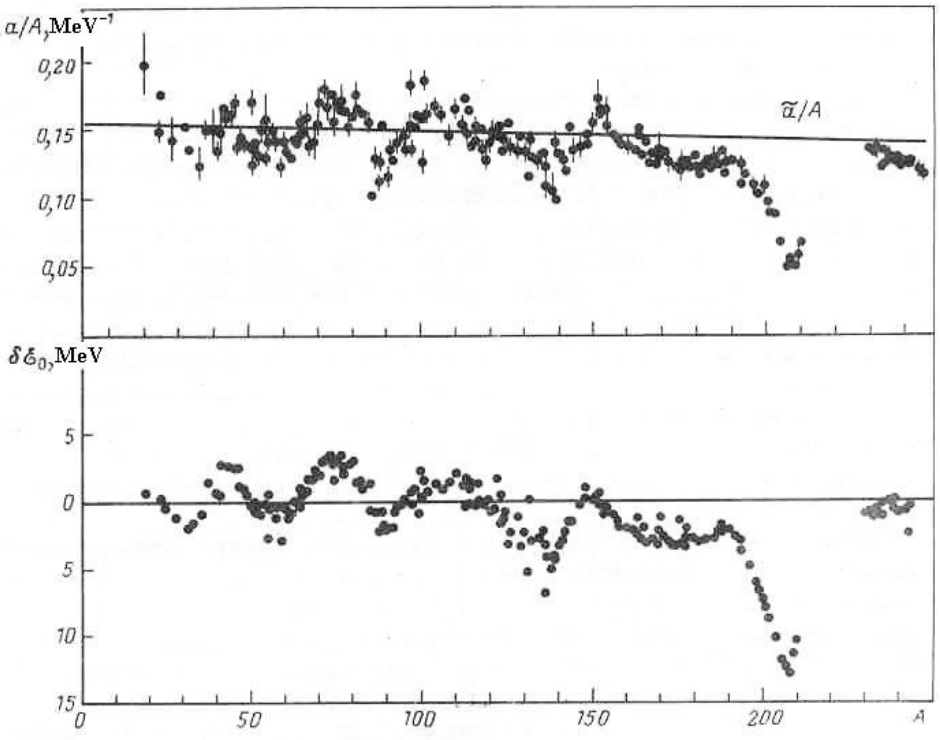

Fig. 4. Ratio of the Fermi-gas level density parameter to the mass number (upper plot) and the shell corrections to the nuclear mass formula (bottom plot)

mass formula calculated for the equilibrium nuclear deformations β [67M]. The strong correlation of the shell corrections and the ratio *a/A* should be considered as a direct evidence of the important role of shell effects in the description of level densities and other statistical characteristics of excited nuclei.

Data on the cumulative numbers of low-lying nuclear levels are also very important for the level density analysis. Many years ago it has been noted [60E, 65G] that the observed energy dependence of the cumulative number of levels is described rather well by the function

$$N(U) = \exp\left[(U - U_0)/T\right], \tag{3.7}$$

where U_0 and T are free parameters determined by the fitting to corresponding data. The quantity $N(U)$ is related to the level density by the relation

$$\rho_{lev}(U) = \frac{dN}{dU} = \frac{1}{T}\exp\left[(U - U_0)/T\right] \quad , \tag{3.8}$$

and it is obvious that the parameter T corresponds simply to a nuclear temperature. Since the value of this parameter is assumed to be constant over the energy range considered, Eq. (3.8) are called the constant temperature model.

In order to obtain a description of the level density for the whole range of excitation energies the low-energy dependence (3.8) should be combined with the high-energy dependence predicted by the Fermi-gas model. The link between both models' parameters can be found from the condition of continuity for the level density and its first derivative at some matching energy

$$U_x = U_0 + T\ln\left[T\rho_{fg}(U_x)\right] \quad , \qquad \frac{1}{T} = \sqrt{\frac{a}{U_x^*}} - \frac{3}{2U_x^*} \quad , \tag{3.9}$$

where U_x^* is the effective matching energy that includes the even-odd corrections (3.5). An analysis of experimental data within the framework of this phenomenological approach has been carried out in Refs. [3, 6], and the obtained parameters are shown in Fig. 5. The values of U_x determine the energies below which the level density description in terms of the Fermi-gas model becomes unsatisfactory, and one can see that for the majority of nuclei this energy is rather high.

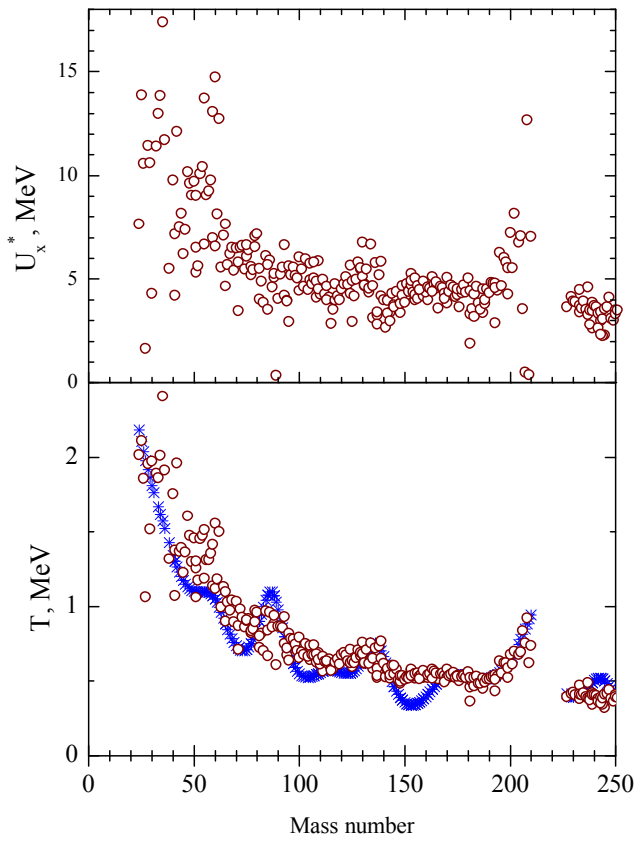

Fig. 5. Mass-number dependence on the nuclear temperature T and the effective excitation energy U_x, bellow of which the level density approximated with the constant temperature model. Blue crosses show the results of the independent analysis of the low-lying discrete levels.

Another approach to the problem of simultaneous description of neutron resonance densities and low-lying levels was proposed in Ref. [73D]. It has been assumed that both sets of experimental data can be described on the basis of the Fermi-gas relations if the level density parameter a and the excitation energy shift δ_{eff} are considered as free parameters for each nucleus. Since for odd-odd nuclei the displacement thus found is negative, the above approach has been called as the back-shifted Fermi-gas model. All data available on the neutron resonance densities and low-lying nuclear levels were analyzed, and parameters a and δ_{eff} have been estimated for the entire mass region. Due to another determination of effective excitation energies the values obtained for the a-parameter are naturally somewhat lower then those shown in Fig. 3. However, the shell effects in the mass dependence of a-parameters remain essentially invariable.

For many nuclei the available experimental data on the spins of low-lying levels can be used to analyze the statistical distribution of angular momentum. The distributions obtained agree rather well with predictions of the Fermi-gas model, but uncertainties of the spin-cutoff parameter estimations are still large for most nuclei.

The results of all consistent microscopic calculations of the nuclear level densities display the damping of the shell effect at high excitation energies [70I, 70R, 83I, 96G]. To include the shell effect damping into consideration the level density parameters should be energy dependent. This dependence may be approximated by the formula [75I]

$$a(U,Z,A) = a_{as}(A)\left\{1+\frac{\delta E_0}{U}\left[1-\exp(-\gamma U)\right]\right\} \quad , \qquad (3.10)$$

where a_{as} is the asymptotic level density parameter to which $a(U)$ tends for high excitation energies and γ is the damping parameter. From a fit of a-parameters with the Myers-Swiatecki shell corrections the following coefficients (in MeV^{-1}) have been obtained: $a_{as} = 0.0959A+0.1468A^{2/3}$, $\gamma = 0.325/A^{1/3}$. The systematics based on the similar formulas have been developed in Refs. [75I, 80K, 94M] and main differences between the corresponding level density parameters relate to estimations of the shell corrections.

On the basis of above results we can conclude that the Fermi-gas and constant temperature models provide us with comparatively simple and convenient formulas for parametrizing experimental data on nuclear level densities. However, these models do not give any explanation for the shifts of excitation energies and shell changes of the level density parameters. An interpretation of these effects must be obtained on the basis of more rigorous models that take into consideration shell inhomogenities of single-particle level spectra, on the one hand, and the superfluid and collective effects produced by the residual interaction of nucleons, on the other. A detailed discussion of such models can be found in the monograph [83I]. However, rigorous microscopic methods of level density calculations are extremely laborious and this severely limits their

application to experimental data analysis. For this reason there is a need to have the level density description, which take into account the basic ideas of microscopic approaches concerning the structure of highly excited nuclear levels while being sufficiently simple and convenient for broad application.

The level density calculations discussed above are based on a consideration of the total energy of an excited nucleus as the sum over all possible combinations of quasi-particle energies. If we include into these combinations all possible rotational or vibrational excitations then the level density of a excited nucleus may be written in the form

$$\rho(U) = \rho_{qp}(U) K_{vibr} K_{rot} \quad , \tag{3.11}$$

where ρ_{qp} is the level density due to quasi-particle excitations only, and K_{vibr} and K_{rot} are the corresponding enhancement coefficients.

In adiabatic approximation the rotational enhancement of the level density depends from the nuclear shape symmetry and can be written as [74B]:

$$K_{rot} = \begin{cases} 1 & \text{for spherical nuclei,} \\ \Im_{\perp} t & \text{for deformed nuclei,} \end{cases} \tag{3.12}$$

where $\Im_i$ is the moment of inertia relatively to the perpendicular axis. This formula is obtained on the assumption of the mirror and axial symmetry of deformed nuclei. This shape have most stable nuclei of the rare-earth elements ($150 \le A \le 190$) and the actinides $A \ge 230$. For non-axial forms the rotational enhancement of the level density becomes even greater [74B].

The vibrational enhancement coefficient is determined in the microscopic approach by the relation

$$K_{vibr} = \prod_i \left[\frac{1 - \exp\left(-\omega_i^0 / t\right)}{1 - \exp\left(-\omega_i / t\right)} \right]^{g_i} \quad , \tag{3.13}$$

where ω_j is the energy of vibrational excitations, ω_i° is the energies of corresponding quasi-particle excitation and g_i is the degeneracy of such excitations. The presence of quasi-particle energies in Eq. (3.13) reflects some account of non-adiabatic effects in excited nuclei. Due to the symmetry conditions imposed on the nuclear Hamiltonian the rotational and vibrational excitations become connected by some relations in consistent microscopic approach [83I]. As a result the calculated collective enhancement coefficients turn out always reduced in comparison to the adiabatic estimation.

It can readily be seen that the adiabatic estimation of K_{rot} increases the nuclear level densities by a factor of 50-100 compared to the calculations based on quasi-particle excitations alone. The increase of the level density due to vibrational excitations will be appreciable only for low-energy excitations with ω_i < 1-2 MeV.

The influence of pairing correlations of superconductive type on nuclear properties can be characterized by the correlation functions $\Delta_{o\tau}$, which directly determine the even-odd differences in the nuclear binding energies and the energy gap $2\Delta_{o\tau}$ in the spectrum of quasi-particle excitations of even–even nuclei. The critical temperature t_{cr} of the phase transition from a superfluid to a normal state is connected with the correlation function through the relation

$$t_c = 0.567\Delta_0 \quad . \tag{3.14}$$

The excitation energy corresponding to the critical temperature may be written as:

$$U_{cr} = 0.472 a_{cr} \Delta_0^2 - n\Delta_0 \quad , \tag{3.15}$$

where n = 0, 1 and 2 for even-even, odd and odd–odd nuclei, respectively. Above the critical energy the level density and other nuclear thermodynamic functions can be described by the Fermi gas relations, in which the effective excitation energy is defined as

$$U^* = U - E_{cond} \quad . \tag{3.16}$$

Here E_{cond} is the condensation energy that determines a reduction of the nuclear ground state energy due to the pairing correlations:

$$E_{cond} = 0.152 a_{cr} \Delta_0^2 - n\Delta_0 . \qquad (3.17)$$

To take into account the shell effects the energy dependence of the level density parameter should be modified in the corresponding way:

$$a(U,Z,A) = \begin{cases} \tilde{a}(A)\left\{1 + \delta E_0 \dfrac{f(U^*)}{U^*}\right\} \text{ for U} \geq U_{cr} \\ a_{cr}(U_{cr}, Z, A) \; for \; U < U_{cr} \end{cases} \qquad (3.18)$$

Below the phase-transition point (3.15) the expressions for thermodynamic functions of a nucleus are rather complex, and they will not be considered here. The complete expressions can be found in Refs. [79I, 83I]. The differences between the thermodynamic functions of the superfluid model and Fermi-gas model are shown in Fig. 6. The differences are most remarkable for the moments of inertia, and available experimental data about the temperature dependence of the effective moments of inertia for fissioning nuclei give the best evidence for the existence of the corresponding phase transition in excited nuclei [82I].

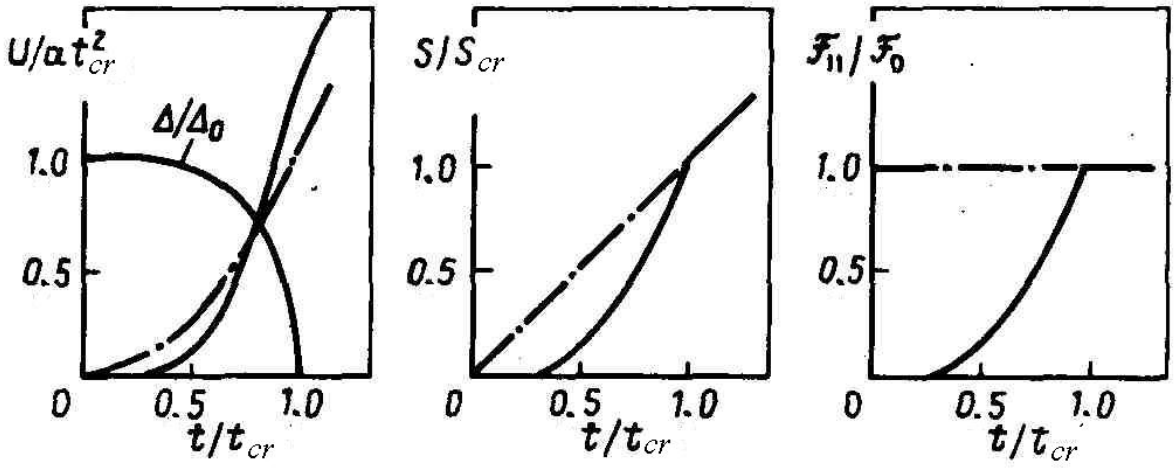

Fig. 6. Temperature dependence of the nuclear thermodynamic functions for the superfluid model (solid lines) and the Fermi-gas model (dashed-dotted corves)

Eq. (3.18) was used as the basic one to construct a phenomenological version of the generalized superfluid model (GSM) [23]. Applying above relations for a description of the pairing correlation effects the level density enhancement coefficients were estimated from the experimental data on the densities of neutron resonances. In such analysis the asymptotic values of the level density parameters were defined as a_{as} = 0.073 A + 0.115 $A^{2/3}$ MeV , the shell corrections were taken from Ref. [67M] and the correlation functions approximated as $\Delta_o = 12/A^{1/2}$ MeV. The coefficients obtained are shown in the upper part of Fig. 7. In the lower part the values of similar coefficients calculated in the adiabatic approximation are given. A correlation of both coefficients is very strong but as a rule the adiabatic evaluations give higher values of coefficients than the similar ones extracted from the observed density of neutron resonances. The difference of these two definitions of the level density enhancement factors demonstrates that the damping of the enhancement coefficients for highly excited nuclei should be taken into account.

At first glance it might seem that the systematics of the level density parameters in terms of the Fermi gas and the GSFM are equally justified, since they give approximately identical description of the level densities at excitation energies close to the neutron binding energy. However, these descriptions correspond deferent absolute values of the level density parameters, because the inclusion of collective effects decreases the *a*-parameters obtained. These reduced values agree well enough with both the experimental data derived from the spectra of inelastically scattered neutrons with energies of up to **7** MeV and the theoretical calculations of the *a*-parameters for the single-particle level schemes of a Woods-Saxon potential [79I, 83I]. This agreement of the data is very

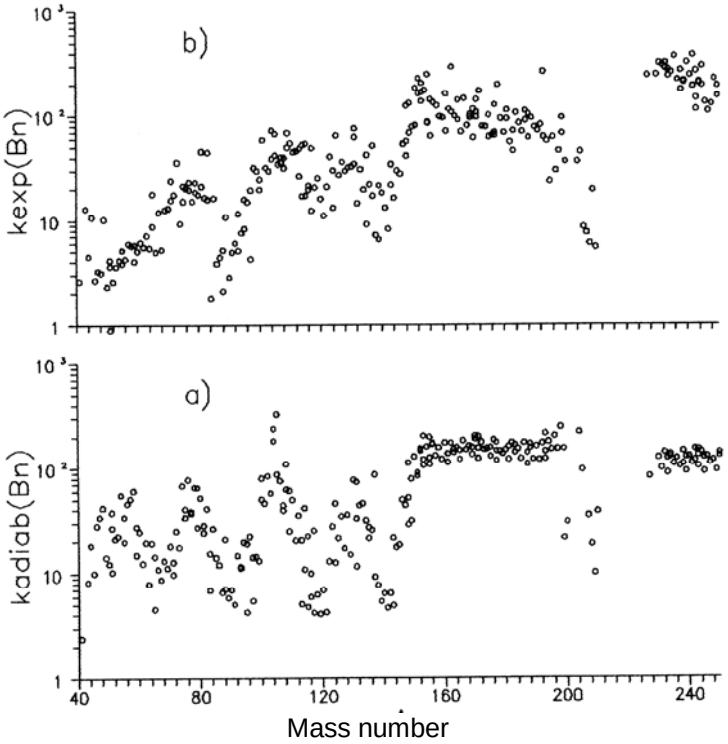

Fig. 7. Collective enhancement factors calculated in the adiabatic approxima-tion (a) and obtained as the ratio of the observed density of neutron resonances to the calculated density of quasi-particle excitations (b).

important, because the evaporation spectra are sensitive precisely to the value of the level density parameter rather than to the magnitude of the excited level density. It is impossible to explain differences between the values of *a*-parameter obtained from resonance data and from evaporation spectra in terms of the Fermi-gas model without account of collective effects. Proper consideration of the level density collective enhancement is also very important for a consistent description of the observed fissilities of highly-excited nuclei [80I].

At first glance it might seem that the systematics of the level density parameters in terms of the Fermi gas and the GSFM are equally justified, since they give approximately identical description of the level densities at excitation energies close to the neutron binding energy. However, these descriptions correspond deferent absolute values of the level density parameters, because the inclusion of collective effects decreases the *a*-parameters obtained. These reduced values agree well enough with both the experimental data derived from the spectra of inelastically scattered neutrons with energies of up to **7** MeV and the theoretical calculations of the *a*-parameters for the single-particle level schemes of a Woods-Saxon potential [79I, 83I]. This agreement of the data is very important, because the evaporation spectra are sensitive precisely to the value of the level density parameter rather than to the magnitude of the excited level density. It is impossible to explain differences between the values of *a*-parameter obtained from resonance data and from evaporation spectra in terms of the Fermi gas model without account of collective effects. Proper consideration of the level density collective enhancement is also very important for a consistent description of the observed fissilities of highly-excited nuclei [80I].

Today it seems almost obvious that in description of the level densities of excited nuclei we should to use the models, which are more consistent than the Fermi-gas, but inevitably more complex. The success of the generalized superfluid model is attributed to the inclusion of the main well-known component of nuclear theory: the pairing correlations, shell effects and collective excitations. Some complexity of the model seems to be justified by the mutual consistency of the parameters obtained from the various experimental data and also by the close relation of the theoretical concepts used to describe the structure of low-lying nuclear levels and the statistical properties of highly excited nuclei.

4 Statistical, direct and valence models of neutron radiative capture

Nuclear reactions involving gamma-rays are usually described in the same way as the reactions with nucleons and other heavy particles in the entrance and exit channels [36B2, 52B2, 58L]. In accordance with the compound nucleus model the neutron radiative capture can be considered as two independent processes: formation of a long-lived excited nucleus by the absorption of neutron and further statistical decay with gamma-ray emission. Primary gamma-rays usually take away only

part of the excitation energy of a compound nucleus and the rest of the energy is taken away by a cascade of gamma-transitions (secondary, tertiary, etc.).

As the interaction between the nucleons and the electromagnetic field is rather weak, general expressions for the probability of radiative transitions can be obtained in terms of standard perturbation theory [52B2]. By expanding the electromagnetic field vector potential into multipole moments we find the following equation for the probability of electric *E1*- or magnetic *M1*-gamma-transitions

$$P_{i\to f}^{El(Ml)} = \frac{8\pi(l+1)}{\hbar l\left[(2l+1)!!\right]^2} k_\gamma^{2l+1} \Sigma \left| \left\langle f \left| Q_{lm}^{E(M)} \right| i \right\rangle \right|^2 \quad , \qquad (4.1)$$

where $k_\gamma = \varepsilon_\gamma/\hbar c$ is the gamma-ray wave number and Q_{lm} is the electric or magnetic multipole operator.

Following N.Bohr's idea about a strong interaction between a neutron and a target nucleus, the initial states in (59) should be identified with the resonance states of the compound nucleus. Due to the complex nature of these states the amplitudes of partial radiative widths should be described by the normal Gaussian distribution (1.19) just like the amplitudes of the reduced neutron widths. In this case partial radiative widths obey to Porter-Thomas distribution (1.20) that is a typical feature of the statistical mechanism of neutron capture.

Experimental test of this distribution for partial radiative widths is a much more laborious task than for neutron widths. Even missing a few of weak gamma-transitions, which are very difficult to measure, could lead to misinterpretations. In general, measurements made for heavy nuclei far off the magic ones show agreement between experimental results and the Porter-Thomas distribution [69C]. The study of the total radiative width distribution is much simpler. As gamma-transitions to many levels of a compound nucleus are permitted for each neutron resonance, the average number of gamma-decay channels in heavy nuclei should be rather large (~ 50÷80). According to (1.21), at large ν fluctuations of total radiative widths are relatively small. This conclusion agrees well with the observed distribution of widths (Fig. 8). The large number of statistically equivalent gamma-decay channels leads to a typical Maxwellian spectrum for gamma-ray energies.

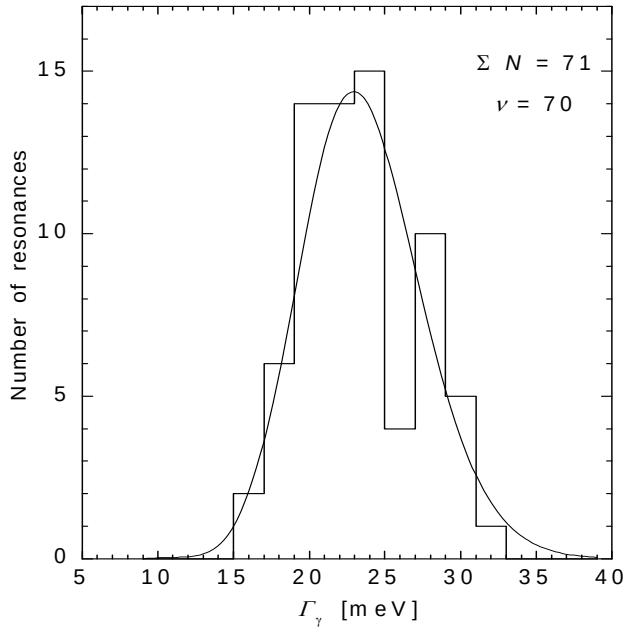

Fig. 8. Total radiative width distribution for the s-wave neutron resonances of ^{238}U

First indications of the existence of non-statistical effects in thermal neutron capture originated from the study of gamma-ray spectra [58G]. For the nuclei close to magic ones very intensive high energy gamma-transitions have been detected which seem to be in contradiction with the Maxwellian spectrum predicted by the statistical model. These experiments brought forth the development of a more rigorous theory of neutron radiative capture, which includes not only statistical but other reaction mechanisms as well.

Basic concepts of the theory have been formulated by Lane and Lynn [60L]. They pointed to the fact that in the application of Eq. (4.1) the full wave function of the neutron scattering problem should be considered for the initial state. This wave function contains all resonance states of a compound nucleus in the internal region as well as the full set of channel states determining the relative motion of a nucleus and neutron in the external region. The presence of non-resonance components, describing the potential neutron scattering in wave functions of the entrance channel and channels of inelastic scattering, brings

forth the corresponding components for the electromagnetic transition probability. Hence in the general case the elements of *S*-matrix for the radiative neutron capture have to be written as

$$S_{n\gamma} = S_{n\gamma}^{pot} + S_{n\gamma}^{res} \quad . \tag{4.2}$$

The resonance component of the matrix elements may be described by the multilevel Breit-Wigner formula

$$S_{n\gamma}^{res} = i \exp\left[-i(\varphi_n + \varphi_\gamma\right] \sum_r \Gamma_{rn}^{1/2} \Gamma_{r\gamma}^{1/2} (E - E_r + i\,\Gamma_r/2)^{-1} \quad . \tag{4.3}$$

However, it should be borne in mind that radiative width amplitudes contained contributions both from the internal resonance and external channel regions. So in the general case they have to be specified in the form of

$$\Gamma_{\gamma n}^{1/2} = \left(\Gamma_{r\gamma}^{inter}\right)^{1/2} + \left(\Gamma_{r\gamma}^{chan}\right)^{1/2} \quad . \tag{4.4}$$

The separation of internal and external regions in the wave functions of scattering problems as well as the definition of the potential and resonance components of *S*-matrix elements depends on the models used in the analysis of neutron cross-sections. Simple estimates of contributions from different components can be obtained from the model of strong interaction between an incident neutron and a target nucleus [60L, 68L]. In this model the neutron is absorbed on the surface of a nucleus and resonance width amplitudes for the decay into any channel are determined mainly by the internal region of a nucleus, i.e., by the first term of Eq. (4.4). This term directly corresponds to the statistical model of radiative neutron capture through a compound nucleus that was considered above.

The potential component of the *S*-matrix (4.2) in the strong absorption model is determined by the direct neutron capture from channel states into bound states of the residual nucleus. For s-wave neutron capture accompanied by an electric dipole transition into the bound *p*- state of a neutron in the residual nucleus the following expression for the cross section was obtained in the model considered [60L, 86R]

$$\sigma_{n\gamma}^{pot} = \frac{0.062}{R\sqrt{E_n}} \left(\frac{Z}{A}\right)^2 \frac{\left(2I_f + 1\right)}{6\left(2I_0 + 1\right)} \Theta_f^2 \left[\frac{y\left(y+3\right)}{y+1}\right]^2 \left[1 + \frac{R - R'}{R} y \frac{y+2}{y+3}\right]^2 \quad , \tag{4.5}$$

where R is the effective radius of the nucleus, R' is the equivalent radius of the potential scattering, θ_f is the spectroscopic factor of the final state which coincides with the spectroscopic factor of the direct (d,p)-reactions, $y^2 = 2m\varepsilon_\gamma R^2/\hbar^2$. The numerical coefficient in Eq. (4.5) holds for the neutron energy in electron-volts and the capture cross section in barns. Initially an additional coefficient taking into account the target spin effects was included into Eq. (4.5), but it was removed after more careful consideration of the formula [86R].

The channel component of the radiative widths of s-resonances can be calculated in a similar way for the strong absorption model [60L]

$$\Gamma_{\gamma i \to f}^{chan} = \frac{16\pi}{9} k_\gamma^3 \Theta_i^2 \Theta_f^2 \left(\frac{Ze}{A}\right)^2 \left(\frac{y+2}{y+1}\right)^2 \frac{R^2}{y} S_{JiJf} \quad , \tag{4.6}$$

where $\theta_i^2 = \Gamma_{ni}/2kRP_l\Gamma_{\rm sp}$ is the ratio of the reduced resonance neutron width to the single-particle width $\Gamma_{\rm sp} = \hbar^2/mR^2$; S_{IiIf} is the geometric factor determined by the angular momenta addition rules.

As the cross-sections of direct capture (4.5) and the channel component of radiative widths (4.6) depend on the spectroscopic factors θ_f, both capture mechanisms should be best revealed for the near-magic nuclei, the low-lying single-particle levels of which have the maximum values of $\theta_f \approx 1$. Of course the problem of identification of each capture mechanism arises. To do that we can analyze the capture cross sections far off resonances on the basis of the theoretical predictions (4.6). On the other hand, in order to differentiate between the two mechanisms we can use the differences in the energy dependence of gamma-transition intensities. For the direct capture the intensity is proportional to ε_γ, whereas for the channel capture it is proportional to ε_γ^2. It was shown in Ref. [78M] through the use of these features that the direct capture mechanism makes an essential contribution to thermal neutron capture cross sections for many nuclei of the region $A \le 50$.

The distribution of partial cross-sections of thermal neutron capture by ^{42}Ca can be considered as one of the best evidence of the direct capture model [79M1]. The distribution observed is shown in Fig. 9 in comparison with the results calculated for available independent data on the spectroscopic factors of the (d,p)-reaction. A similarly good agreement with theoretical estimations was also demonstrated for partial cross sections of thermal neutron capture on ^{130}Te, ^{136}Xe, ^{138}Ba [79M1]. Rather complete reviews of experimental data available about the direct capture of thermal and low-energy neutrons can be found in Refs. [79M2, 83A] which also discuss the agreement of experimental data with the theoretical models more rigorous than the strong absorption model.

Analyzing the channel component of the radiative resonance widths Lynn proposed to consider the corresponding transitions as changes of the valence neutron states separated from the full spectrum of more complicated nuclear excitations instead of dividing the internal and external regions in the neutron wave function [68L]. In such an approach the relation determines the partial widths of electrical dipole transitions

$$\Gamma_{\gamma i\to f}^{val} = \frac{16\pi k_\gamma^3}{9}\Theta_i^2\Theta_f^2\left(\frac{Ze}{A}\right)^2\left|\int_0^\infty u_i u_f r dr\right|^2 S_{JiJf} \quad , \qquad (4.7)$$

where u_i and u_f is the single-particle neutron wave functions for the initial and final states. The initial calculations used the wave functions of the shell model single-particle potential and the estimation of the single-particle width Γ_{sp} corresponded to the strong absorption model. As the single-particle width for the realistic shell-model potential with a diffuse range is several times larger, problems arise in matching the single-particle widths to the normalization of single-particle wave functions.

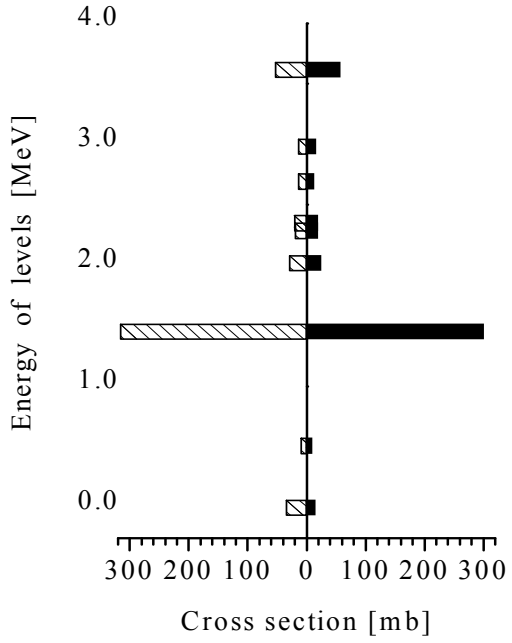

Fig. 9. Comparison of the observed partial cross sections of the thermal neutron capture on ^{42}Ca (left) with direct capture model calculations (right) [79M1]. The energies of excited levels are given on the left.

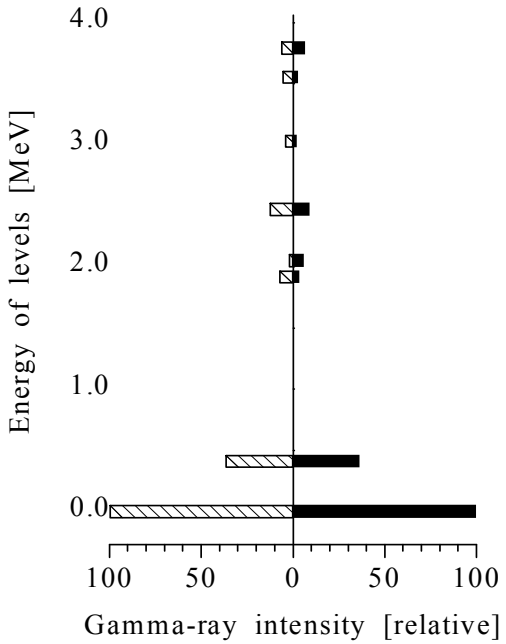

Fig. 10. Comparison of the relative intensities of observed partial radiative widths for the *s*-wave neutron resonance on ^{54}Fe at the energy of 7 keV (left) with the valence capture model predictions (right) [80R].

A more rigorous approach to the calculations of the valence neutron capture was formulated by Lane and Mughabghab within the framework of the optical model [74L]. They obtained the following relation for the valence component of radiative widths

$$\Gamma_{\gamma i\to f}^{val} = \frac{16\pi k_\gamma^3}{9}\Theta_f^2\left(\frac{Ze}{A}\right)^2\Gamma_{ni}\left|\frac{\mathrm{Im}\left\langle u_f|r|u_i^{opt}\right\rangle}{\mathrm{Im\,tg}\,\delta_{opt}}\right|^2 S_{JiJf} \quad , \qquad (4.8)$$

which, unlike (4.7), contains the single-particle wave function u_i and phase shift δ_{opt} of the optical model. As a result of the mutual reduction of factors related to the single-particle wave function normalization and an increase in single-particle widths, predictions made according to the optical model (4.8) do not differ essentially from the initial estimations of valence widths with Eq. (4.7) in the vicinity of 3p-giant resonance ($A \sim 90$). However, the optical model calculations yield width values 1.5...2 times higher than (4.7) in the region of 3*s*-resonance ($A = 50...70$) [75B1, 78M]. The calculations of the radiative width valence components for a wide range of mass numbers, as well as the energy changes in the widths are reviewed rather completely in Ref. [78A].

The analysis of partial radiation widths of s-wave resonances in ^{96}Zr and ^{98}Mo was one of the first quantitative tests of the valence neutron capture model [71M]. Further studies yielded similar results for many nuclei in the vicinity of 2*p*-, 3*s*- and 3*p*-giant resonances [78A, 80R, 83A]. The distribution of the partial radiation widths obtained for the s-wave neutron resonance at the energy of 7 keV on ^{54}Fe (Fig. 10) may be considered as a bright example of a good agreement of theoretical predictions with experimental data [80R].

The valence neutron radiative capture was also analyzed in the semi-microscopic approaches based on the modern multi-particle shell model [75C, 77U]. The results obtained do not differ significantly from those obtained through the optical model. However, they help to identify the optimum criteria for the selection of the optical model parameters and to achieve a more consistent description of nuclear structure effects in neutron induced reactions.

As the valence component of radiative widths is directly proportional to single-particle spectroscopic factors of initial and final states, the valence neutron capture should entail correlations of partial radiative widths for different neutron resonances as well as correlations between neutron and radiative widths. Such correlations were used in Ref. [78A] to estimate the contribution of the valence capture into the total radiative widths for a wide range of nuclei. For light and medium nuclei with a closed neutron shell these contributions may reach 20-30%, however, they decrease sharply with distance from the magic numbers.

It should be noted that the valence capture model explains correlations of widths caused by single-particle effects only. Experimental data on many nuclei reveal correlations of partial radiative widths, which can be explained by a non-statistical distribution of amplitudes of more complicated entrance excitations [71L, 80B1]. Noncontradictive description of such excitations seems to be feasible in the framework of consistent microscopic approaches. The quasiparticle-phonon model seems a rather promising one [78S]. It allows interpreting not only the single-particle valence neutron correlations, but also those related to collective nuclear excitations. A detailed discussion of the results of this model as well as the corresponding analysis of experimental data can be found in [79S, 80B1, 83A].

The description of radiative widths can be made more consistent if in accordance with the general methods of the statistical theory of nuclear reactions we relate the gamma-decay widths to the cross section of the inverse absorption reaction. The absorption cross section of gamma-ray by an unexcited nucleus, averaged over resonances, can be written as

$$\overline{\sigma}_{\gamma}^{0}(\varepsilon_{\gamma}) = \pi\left(\frac{\hbar c}{\varepsilon_{\gamma}}\right)^{2} g_s \frac{1}{\Delta E}\int_{\varepsilon_{\gamma}-\Delta E/2}^{\varepsilon_{\gamma}+\Delta E/2} dE' \sum_r \frac{\Gamma_{\gamma r}^{0}\Gamma_r}{(E'-E_r)^2+\Gamma_r^2/4} = 2g_s\left(\frac{\pi\hbar c}{\varepsilon_{\gamma}}\right)^{2}\frac{\left\langle \Gamma_{\gamma}^{0}\right\rangle}{D_i} \quad , \qquad (4.9)$$

where $g_s = (2I_i + 1)/2(2I_0 + 1)$ is the statistical weight factor determined by the spins of initial I_o and excited I_i states and $\langle\Gamma_{\gamma}^{o}\rangle$ is the average width of radiative decay to the ground state. Eq. (4.9) is valid also for the absorption cross section of gamma-rays by an excited nucleus. However, in that case the radiative widths for the corresponding excited state should be substituted in the right-hand side of the equation. Assuming that the photo-absorption cross section does not depend on the initial state of the nucleus and is determined only by the energy of the gamma-quanta, the average width of the gamma-decay of the excited nucleus to any lower state can be written as

$$\left\langle \Gamma_{\gamma i\to f}^{El}\right\rangle = \frac{\varepsilon_{\gamma}^{2} D_i(U)}{2g_s(\pi\hbar c)^2}\overline{\sigma}_{\gamma}^{0}(\varepsilon_{\gamma}) \quad . \qquad (4.10)$$

This expression is usually referred to as the Brink hypothesis [55B].

For dipole electric transitions the absorption cross section observed has a shape of a giant resonance. Approximating such a cross section with the Lorentz curve we obtain the following relation for the radiative width

$$\left\langle \Gamma_{n\to f}^{E1} \right\rangle = \frac{D_i(U)}{3(\pi\hbar c)^2} \frac{\varepsilon_\gamma^4 \Gamma_g^2 \sigma_g}{\left(\varepsilon_\gamma^2 - E_g^2\right)^2 + \varepsilon_\gamma^2 \Gamma_g^2} \quad , \tag{4.11}$$

where E_g is the energy of the giant resonance, Γ_g is its half-width and σ_g is the resonance value of the photo-absorption cross section. It was shown by Axel [62A] that for gamma-ray energies close to the neutron binding energy Eq.(75) can be replaced with a rather simple formula

$$\left\langle \Gamma_{n\to f}^{E1} \right\rangle = k_{E1}^A A^{8/3} \varepsilon_\gamma^5 D_i(U) \tag{4.12}$$

with the factor of $k_{E1} = 6.1\cdot10^{-15}$ MeV^{-5} corresponding to the mean parameters of the giant resonance: $E_g = 80/A^{1/3}$ MeV, $\Gamma_g =$ 5 MeV, $\sigma_g = 230$ mb.

Most direct experimental information on the electromagnetic transitions in highly-excited nuclei is provided by the measurements of partial radiative widths of neutron resonances. Since partial widths fluctuate from resonance to resonance, averaging the observed widths over a sufficiently large number of resonances is necessary for a comparison with the above estimations. Such data are usually represented as the reduced gamma-ray strength functions determined as

$$k_{E(M)l} = \frac{\left\langle \Gamma_{n\to f}^{E(M)l} \right\rangle}{\varepsilon_\gamma^{2l+1} D_i(U)} \tag{4.13}$$

For dipole electric transitions the definition of strength functions based on Eq. (4.12) is also widely used. Available experimental data on the radiative strength functions for gamma-ray energies close to the neutron binding energy are shown in Fig. 11.

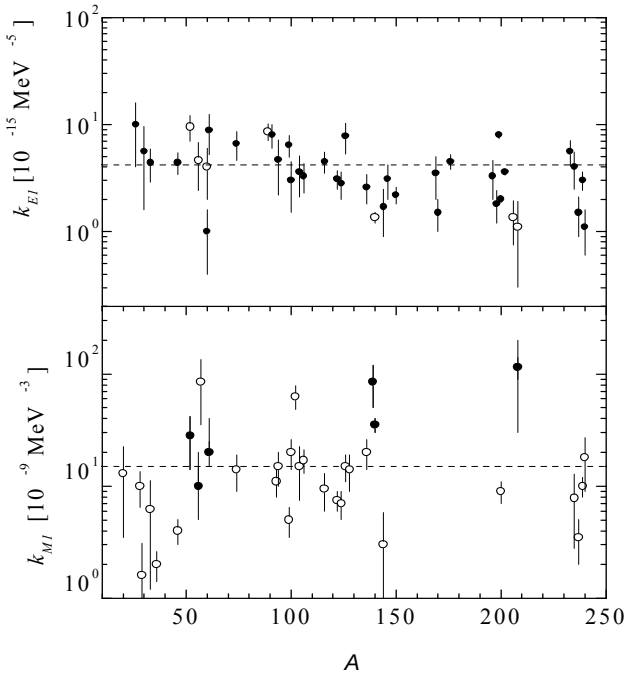

Fig. 11. Dependence of *E1* (a) and *M1* (b) gamma-ray strength functions on mass number. Experimental points obtained from observed partial radiative widths of neutron resonances in (n,γ)- and (γ,n)-reactions averaged over resonances [81C], the dashed lines correspond to strength function estimations (4.14).

On the average these data correspond to the following values of gamma-ray strength functions [81C]:

$$k_{E1}^A = (4.2 \pm 0.4)\cdot10^{-15}\cdot A^{8/3} \quad \text{MeV}^{-5}, \tag{4.14}$$
$$k_{M1} = (1.6 \pm 0.4)\cdot10^{-8} \quad \text{MeV}^{-5} \quad .$$

A considerable dispersion of the data in Fig. 7 relative to the average values is displayed, especially for magnetic transitions. Errors of strength function evaluations are also big for many nuclei because of the limited number of resonances.

Methods of direct measurements of the partial radiative widths averaged over many resonances are very promising in the study of gamma-ray strength functions [70B]. Such measurements demonstrated that strength functions of dipole electric transitions observed for rareearth nuclei within the range of gamma-ray energies from 6 to 8.5 MeV approximately correlate with the Axel-Brink model. The giant resonance with the energy of 8...9 MeV was also observed in the gamma-ray strength functions of the dipole magnetic transitions [72B, 86C]. The estimation of the gamma-ray strength functions for quadrupole electric transitions was obtained in this approach too [86C]

$$k_{E2} = (1...3)\cdot10^{-14}\cdot A^{4/3} \quad \text{MeV}^{-5} \tag{4.15}$$

Experimental data on the gamma-ray continuous spectra produced in absorption of thermal and resonance neutrons as well as the gamma-ray spectra released in (d,pγ)-reactions are also widely used for the analysis of the energy dependence of radiative strength functions [74B]. Strength functions of the dipole electric transitions obtained for ^{181}Ta and ^{198}Au from the description of observed spectra are shown in Fig. 12 together with the results of partial widths analysis. Data available for the deformed nucleus ^{181}Ta are in comparatively good agreement with the Lorentzian parameterization of the photo-absorption cross sections in the whole range of gamma-ray energies. At the same time considerable deviations from the Lorentzian curve appear for the spherical nucleus ^{198}Au at gamma-ray energies below 5 MeV.

Similar discrepancies manifest themselves for many nuclei within the ranges of mass numbers $110 < A < 140$ and $190 < A < 210$. The anomalous "gross-structure" in the high-energy part of the gamma- ray spectrum produced in the (n,γ) and (d,pγ)-reactions is directly related to these discrepancies [74B]. An increase in the deviation of the giant resonance tail from Lorentzian parameterization for mass numbers close to magic ones was also observed in the gamma-ray strength functions obtained from the direct averaging of partial radiative widths of neutron resonances [82R].

Unique possibilities to study the gamma-ray strength functions at energies below 1.5 MeV are offered by the investigation of the (n,γα)-reaction [82P]. The strength functions of the dipole electric transitions obtained from the analysis of the ^{143}Nd(n,γα)-reaction are shown in Fig. 13 together with the results of the analysis of averaged partial radiative widths for the gamma-ray energies of 5...7 MeV [82R] and data on the photo-absorption cross sections in the energy range above 8 MeV [71C]. The Lorentz curve which gives a good description of the photo-absorption cross sections passes much higher than the neutron resonance data on gamma-ray strength functions at energies of 5...7 MeV and fails to describe the energy dependence of the (n,γα)-data below 1.5 MeV. Unfortunately, such manifold experimental data are currently available only for one nucleus,

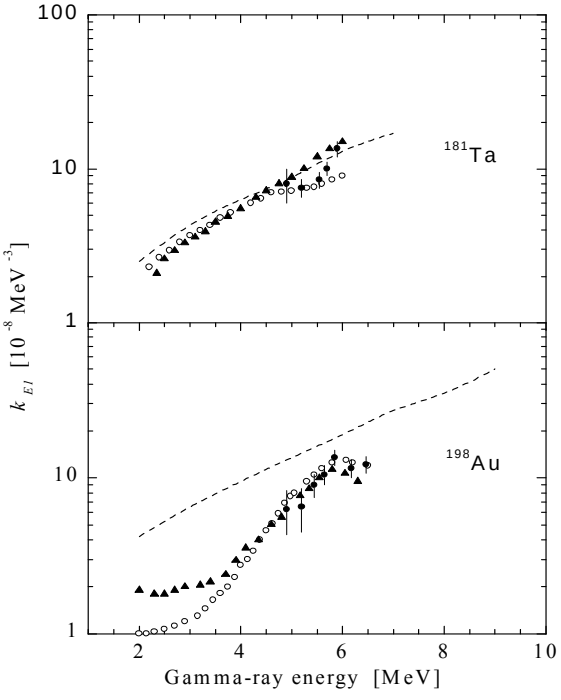

Fig. 12. Energy dependence of gamma-ray strength functions obtained from the analysis of partial radiative resonance widths (•), from the gamma-ray spectra of the thermal neutron capture reaction (o) and the (d,pγ)-reaction (▲) [74B]. Dashed curves correspond to Lorentzian parameterization of the giant dipole resonance.

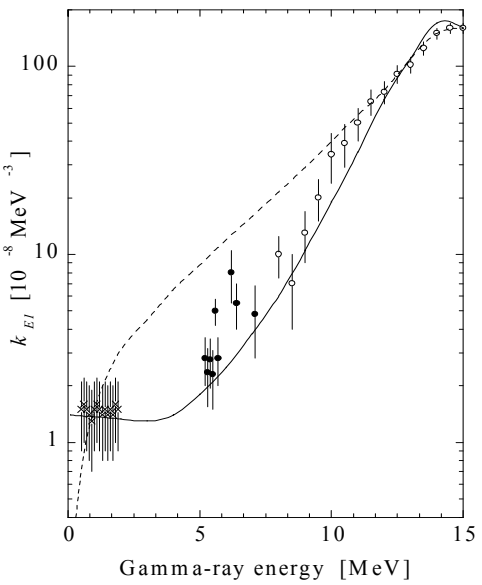

Fig. 13. Energy dependence of gamma-ray strength functions of ^{144}Nd obtained from photo-absorption cross sections (o), from averaged partial widths of neutron resonances (•) and from the analysis of the (n,γα)-reaction (×). The dashed curve corresponds to the traditional Lorentzian approximation of the photo-absorption cross section; the solid curve is the Lorentzian approximation with the width dependent on gamma-ray energy and temperature of the residual nucleus [83K].

^{144}Nd. Therefore, it is difficult to understand to what extent the observed deviations from the standard Lorentzian shape reflect individual features of the given near-magic nucleus and how deviations will change if one moves away from the closed neutron shell.

To interpret the observed decrease in the radiative strength functions in the giant resonance tail region it was proposed in Refs. [82B, 83K] to use the giant resonance widths those depend on both the gamma-ray energies and temperature of an excited nucleus. Such dependence should be similar to the formulas for the zero sound attenuation in the Fermi-liquid theory [57L] and may be approximated in the following form

$$\Gamma_g(\varepsilon_\gamma, t) \approx \left(\frac{\Gamma_g}{E_g^2}\right)^{\exp} \left(\varepsilon_\gamma^2 + 4\pi^2 t^2\right) \quad , \tag{4.16}$$

where E_g and Γ_g are the observed energy and half-widths of the giant dipole resonance and t is the temperature of the residual nucleus. Such modification of Eq. (4.11) gives a good description of the strength functions obtained from the partial radiative widths of neutron resonances and the temperature dependence of the giant resonance width (4.16) is of principal importance to the explanation of the radiative strength functions at gamma-ray energies below 1.5 MeV (Fig. 13). The generalized Lorentzian model that includes the energy and temperature dependence of the giant resonance width have got further development in Ref. [84U, 85K, 90K], where the formulas for gamma-ray strength functions of *E1*, *E2* and *M1*-transitions were discussed in detail and global systematics of its parameters were proposed.

Besides the data on partial radiative widths for neutron resonances, considerably more extensive information exists on total radiative widths. These widths are one of the main characteristics of statistical description of neutron radiative capture cross sections and much attention was paid to their systematization and analysis. Since the dominant contribution to radiative widths is made by electrical dipole transitions, the relation for the total widths can be written in the form of

$$\Gamma_\gamma^{tot}(B_n, J) = \sum_{I=|J-1|}^{J+1} \int_0^{B_n} \varepsilon_\gamma^3 k_{E1}(\varepsilon_\gamma) \frac{\rho(B_n - \varepsilon_\gamma, I)}{\rho(B_n, J)} d\varepsilon_\gamma \quad . \tag{4.17}$$

If necessary, contributions of the magnetic dipole transitions to total radiative widths can be taken into account using similar relations.

The gamma-transitions with energies about 2...3 MeV play a decisive role in the integrated function Eq. (4.17). For such transitions the Lorentzian approximation of the giant dipole resonance tail can be presented as rather a simple function

$$\frac{\left\rangle \Gamma_{\gamma i \to f}^{E1} \right\langle}{D_i} = 1.6 \cdot 10^{-5} \left(\frac{\varepsilon_\gamma}{7MeV}\right)^4 \left(\frac{A}{100}\right)^{7/3} \quad . \tag{4.18}$$

Using this parameterization for gamma-ray strength functions and the constant temperature model for the level density we can obtain the following relation for total radiative widths

$$\Gamma_\gamma^{tot} = 10^{-5} A^{7/3} (t/\mathrm{MeV})^5 \quad , \tag{4.19}$$

where the numerical factor corresponds to the widths in meV. Application of other functional representations of gamma-ray strength functions and nuclear level densities will produce only some changes in the power dependence of the total radiative widths on the temperature and mass number [81M, 82B, 83M]. As an empirical systematics of the radiative widths dependence on the mass number and excitation energy of the excited nucleus the following relation was suggested in Ref. [83M]

$$\Gamma_\gamma^{tot} = 0.0321 A^{-0.823} \left(B_n / MeV\right)^{2.56} \quad . \tag{4.20}$$

Beside simple analytical estimations, more accurate numerical calculations of the total radiative widths were performed, in which the individual variations of the nuclear level densities and gamma-ray strength functions were taken into account [77J, 80R, 82H, 90K]. Results of these calculations provide a sufficiently good description of the main variations observed in the total radiative widths of neutron resonances. In particular, they explain some systematic differences of the total radiative

widths for s- and p-wave neutron resonances in the mass range $90 < A < 110$ as an effect of the domination of certain parity in the spectra of low-lying nuclear levels.

It should be noted that the main part of some discrepancies of statistical calculations of total radiative widths with experimental data relates to near-magic nuclei. As discussed above , significant contribution to radiative widths of such nuclei may arise from different non-statistical effects and, the first of all, from the valence mechanism of the neutron radiative capture. The valence neutron capture model provides good explanation the difference between the radiative widths of s- and p-wave resonances at mass numbers about 50 and 90 which are not described by statistical calculations [78A, 80R]. For the near magic nuclei an important role in the analyses of radiative widths can play the shell effects similar to the shown one in Fig. 13. Unfortunately, limited experimental information on the gamma-ray strength functions and the valence component of neutron resonance widths does not allow us to identify all uncertainties of theoretical model parameters used in different descriptions of total radiative widths.

For the neutron radiative capture the Hauser-Feshbach-Moldauer relation (2.10) can be written in the form

$$\sigma_{n\gamma} = \pi\lambda\!\!\!^{-2}_{n} \sum_{J,l,j} g_J T^{J\pi}_{lj}(E_n) \frac{T^{J\pi}_{\gamma c}(E_n) F^{J\pi}_{lj\gamma}(E_n)}{T^{J\pi}_{\gamma}(E_n) + \sum_{n'l'j'} T^{J\pi}_{l'j'}(E_{n'})} \qquad (4.21)$$

were T_γ are the radiative transmission coefficients connected with the radiative widths through the relation

$$T^{J\pi}_{\gamma}(E_n) = 2\pi\Gamma^{J\pi}_{\gamma}(B_n + E_n) / D^{J\pi}(B_n + E_n) \qquad (4.22)$$

Because the excitation energy of a residual nucleus after the emission of low-energy gamma-quants can be above the neutron binding energy and the reactions of (n,γn′),…, (n,xγn′) can be possible, the numerator of Eq. (4.21) includes only the capture radiative coefficients corresponding to the reaction channals without the secondary emission of neutrons.

The available experimental data on the radiative capture of fast neutrons have been analysed by many authors [60B, 69M, 70S, 80R, 86B]. An effect of different factors on the calculated cross sections can be traced in Fig. 14, where the statistical model calculations are compared with the experimental data for the ^{68}Zn(n,γ) reaction. Contributions of the various partial waves change rather quickly with the increasing of a neutron energy and the relative contributions depend essentially on the corresponding neutron strengh functions. For the neutron energies below the first excited level of the taget nucleus the fluctuation correction (2.24) reduces the calculated cross section by 15-25%. For higher energies, when several inelastic scattering channels are open, the

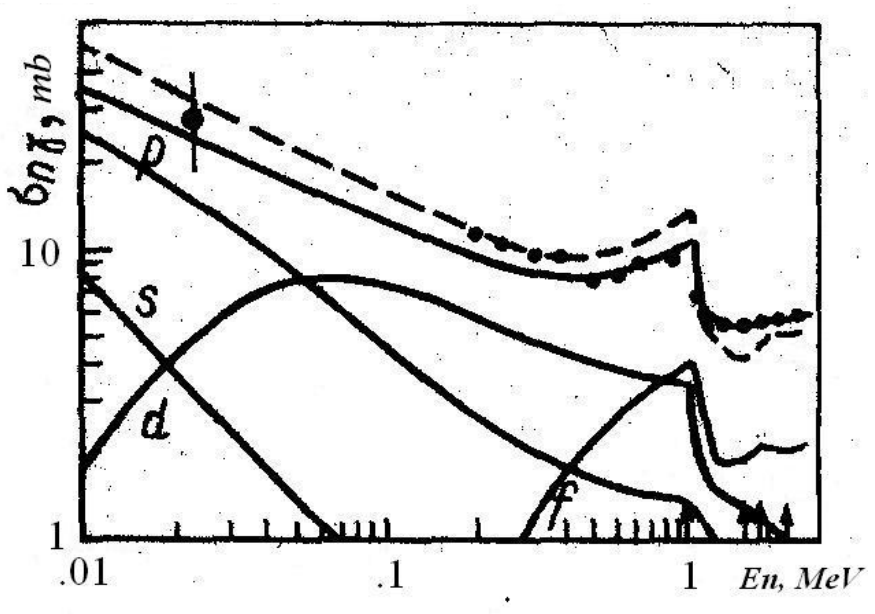

Fig. 14. Neutron capture cross sections for ^{68}Zn, calculated taking into account the width-fluctuation corrections (solid curves) and without such corrections (dashed curve). The contributions of various partial waves are shown together with the corresponding experimental data for the total capture cross section (●).

fluctuation corrections lead to a redistribution of partial wave contributions on account of which the total capture cross section can even increase. With the subsequent increase of a number of open inelastic channels the effects of fluctuation corrections disappear rather quickly. On the other hand the energy dependence of the radiative strengh functions and the nuclear level densities begins to effect inceasingly on the calculated results with a growth of the incident neutron energy.

5 Nuclear fission

The main concepts of the nuclear fission description developed by N. Bohr, Wieler [39B] and Frenkel [39F] are based on the liquid drop model. According to this model the competition of the surface tension forces of a drop of the nuclear liquid and the Coulomb repulsion forces related to the nuclear charge lead to the formation of an energy barrier which prevents a spontaneous decay of a nucleus (Fig. 15). The penetrability of the barrier determines the periods of spontaneous fission of nuclei. In the liquid drop model for heavy nuclei the height of the fission barrier quickly decreases with the increase of Z^2/A. At certain $(Z^2/A)_{cr}$ = 46-48 the barrier should disappear. The decrease in height brings forth the exponential increase in barrier penetrability. These changes of barriers are in good agreement with the behavior of the spontaneous fission lifetimes of the actinide nuclei, ranging from the long-lived isotopes of uranium to the artificially synthesized short-lived isotopes of fermium, mendelevium and so on. [55G, 58F2, 83F, 90S].

The height of the barrier also plays a major role in the description of the fission probability of the compound nucleus. For an excited nucleus the fission width Γ_f is determined, as for the neutron or any other decay width, by the product of the excited level spacing D_c and the sum of the transmission coefficients over channels leading to the decay of the fissioning nucleus

$$\Gamma_f(U_c) = \frac{D_c(U_c)}{2\pi} \sum_i T_{fi} \quad . \tag{5.1}$$

As the fission fragments formed have a wide dispersion of masses and excitation energies, in terms of the formal reaction theory we should consider a huge number of fission channels even at low excitations of the parent nucleus. However, if we proceed from the principles of the liquid drop model, the intermediate saddle configuration, which the nucleus goes through at the top of the fission barrier, should be of vital importance for the determination of fission probability. In the saddle point a significant amount of the initial excitation energy is concentrated in the fission degree of freedom. This imposes significant limitations on the excitations of other degrees of freedom. As both the saddle point and the relevant limitations are the same for the whole set of fission fragments, the emission widths of different fragments get in a strong correlation with each other. The total fission width resulting from this correlation is determined by the characteristics of transitions states in the vicinity of the saddle point. Therefore, just these states are usually considered as the fission channels. The spectrum of the fission channels should be similar to the observed level spectra of the heavy deformed nuclei. In particular, if the form of a nucleus in the saddle point is symmetrical both

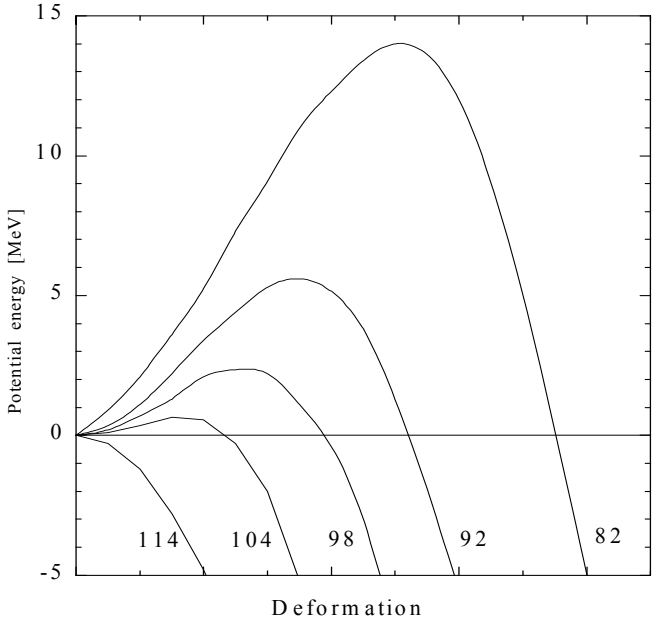

Fig. 15. Fission barriers of heavy nuclei according to the liquid drop model. The charge numbers are given for the corresponding curves.

axially and mirror-like, the same sequences for the angular momentum values J, parities π and the projections K of the angular momentum on the symmetry axis should be realized for the lowest fission channels as for the rotation bands of the ground states of the rare earths and transuranium nuclei [55B1].

To describe the energy dependence of fission widths a simple formula for the penetrability of the parabolic barrier can be used

$$T_i(E) = \left\{1 + \exp\left[\frac{2\pi}{\omega_i}(E_i - E)\right]\right\}^{-1} \quad , \tag{5.2}$$

where E_i is the energy of the transition state; ω_i is the curvature of the corresponding barrier close to its top. In the sub-barrier region the penetrability of the lowest fission channel is the dominating component of the sum (91). Resulting from the exponential growth of the barrier penetrability, which is much stronger than the decrease in the level spacing, the fission width grows exponentially with the increase of the excitation energy of a nucleus. At energies above the barrier the penetrability does not prevent nuclear transitions to open fission channels and the fission width grows due to the growth of a number of open channels only. This growth is much weaker than the sub-barrier increase of width, and this change in the growth rate of fission widths is usually used in experimental data analyses as a direct method for the estimation of fission barrier heights [73V].

The study of angular distributions of fission fragments is of great interest too. To consider the main features of such distributions let us use the semi-classical approach, applied above for the general analysis of the compound reaction angular distributions. For given values of the angular momentum J and its projection on the symmetry axis K permitted directions of fission fragment emission are restricted by the delta-function $\delta(\cos\vartheta_o - K/J)$, where ϑ_o is the angle between the fission axis and the direction J. After averaging the δ-function over possible orientations of J in the compound nucleus we get the following formula [55B1] for the angular distribution of fragments with respect to the beam of particles inducing fission

$$W_{JK}(\Theta) = \begin{cases} 0 & for \sin\Theta < K/J \quad , \\ \dfrac{1}{2\pi^2(\sin^2\Theta - K^2/J^2)^{1/2}} & for \sin\Theta \geq K/J \quad . \end{cases} \tag{5.3}$$

The formula shows that at small K/J fission fragments are concentrated mostly in the region of small front and back angles, whereas at growing K/J the maxima in the angular distribution are shifted towards $\pi/2$ angle. If channels with different J and K can contribute to the angular distribution of fragments, Eq. (93) should be averaged over the distribution of J and K in the corresponding fission channels.

The analysis of the observed fission fragment angular distributions produced by gamma-quanta, neutrons and different charged particles, demonstrated that in a wide range of energies the distribution of the angular momenta projections K on the direction of fission fragments does not differ much from the distribution of K for the fission channels in the saddle point [73V]. This results in the conclusion that there is no essential energy exchange between the rotation and other degrees of freedom during the motion of the fissioning nucleus from the saddle configuration to the scission. For low-energy fission such adiabatic separation of rotation seems to be resulting from the conservation of the axial symmetry of the fissioning nucleus in the process of a relatively slow descent form the barrier top. However, for high-energy fission the reason for the isolation of rotation may be completely different, namely, fast (as compared to the period of rotation) descent from the barrier.

Early studies show that despite some successful results the liquid drop model cannot explain the major peculiarity of spontaneous and low-energy fission of the actinides, namely the asymmetric mass distribution of fission fragments. Further experiments demonstrated that this asymmetry of mass yields is closely related to the increase in the mean kinetic energies of fragments in the asymmetric fission and to the saw-like mass dependence of the average number of neutrons emitted by fission fragments [73V]. All of the above features of the low-energy fission of actinides are

obviously correlated with the position of the heavy magic fragment with the mass number of 130...140. This fact proves the strong influence of shell effects on the fission fragment formation.
Initially it seemed that the above effects can be explained by some modifications of the liquid drop model predictions for the configurations close to the scission point (the point where the fissioning nucleus breaks into two fragments). However, in the 60-s new phenomena were discovered in nuclear fission studies, an explanation of which demanded much more radical changes in the fission model. This refers primarily to the spontaneously fissioning isomers found in the Am isotopes [62P] and to the intermediate resonance structures observed into the neutron induced fission cross sections [67V, 68M], which cannot be interpreted from the point of view of traditional formulas (92) for the fission barrier penetrability.

Calculations of the nuclear deformation energy proved to be the keys to the understanding of these phenomena. They have been made by Strutinsky on the basis of the shell correction method [66S, 68S]. Fission barriers for the actinide nuclei obtained had the form of a two-hump curve with a rather deep potential well between the humps (Fig. 16). The two-hump structure of the fission barrier helps to explain both the nature of the spontaneously fissioning isomers that can be identified with the lowest energy states of the fissioning nucleus in the second potential well and the resonance character of the energy dependence of the two-hump barrier penetrability resulting from the quasi-stationary states of the nucleus in the well [68L, 69B].

To discuss the major features of the two-hump barrier model let us use the quasi-classical equation for the penetrability of the barrier [69I]

$$T(E) = 64 T_A T_B \left\{(16 + T_A T_B)^2 \cos^2\varphi + 16(T_A + T_B)^2 \sin^2\varphi\right\}^{-1} \approx$$
$$\approx \frac{T_A T_B}{4}\left\{\left(\frac{T_A + T_B}{4}\right)^2 \sin^2\varphi + \cos^2\varphi\right\}^{-1} . \qquad (5.4)$$

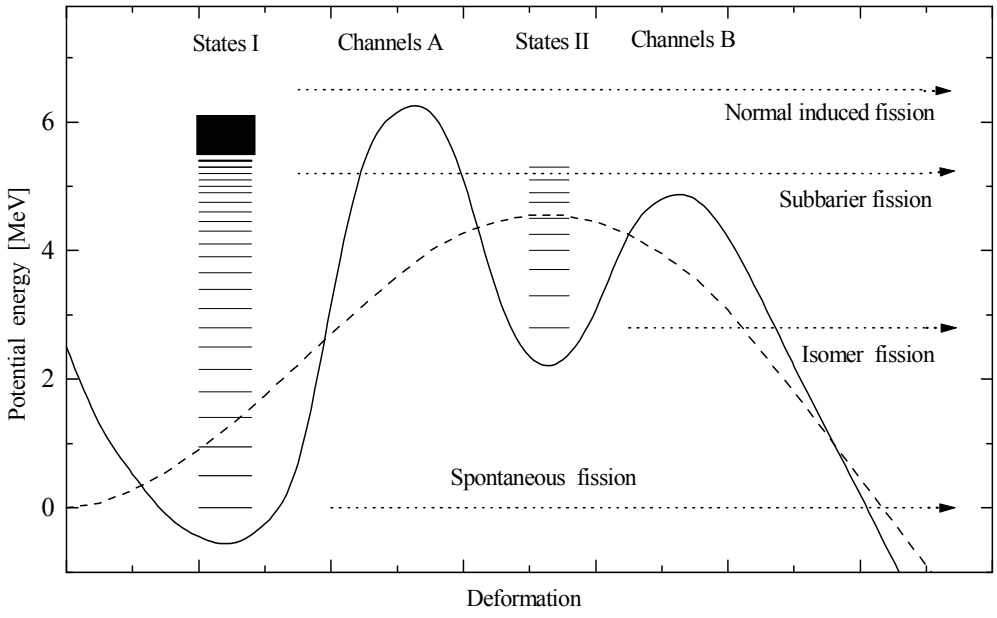

Fig. 16. Fission barriers of actinides in accordance with the shell model calculations

Here T_A and T_B are the penetrability of the humps A and B, respectively, each of which can be described by Eq. (5.2); $\varphi(E)$ is the phase integral determined by the semi-classical quantization conditions for the eigen states in the well between the humps (Fig. 15). In the sub-barrier region the penetrability of the two-hump barrier (94) varies greatly with energy changes reaching top values at energies corresponding to quasi-stationary levels $\varphi(E) = \pi(n + 1/2)$, and reaching minimum values between quasi-stationary levels:

$$T_{\max}(E) = \frac{4T_A T_B}{(T_A + T_B)^2};\ T_{\min}(E) = \frac{T_A T_B}{4} \quad . \tag{5.5}$$

By averaging (5.4) over the interval between the levels we obtain the average penetrability of the two-hump barrier

$$\overline{T}(E) \approx \frac{1}{\pi} \int_{-\pi/2}^{\pi/2} P(\varphi) d\varphi = \frac{T_A T_B}{T_A + T_B} \quad . \tag{5.6}$$

The above model of the one-dimensional potential barrier contains quasi-stationary states only which correspond to vibrational excitations of the nucleus in the potential well formed by two humps. In addition to such collective excitations, the fissioning nucleus at deformations corresponding to the second well should have many other excited states similar to complex many-particle excitations of nuclei at equilibrium deformations. Interaction between the collective and quasi-particle excitations leads to the dissipation of the vibrational excitations, i.e. to the fragmentation of vibrational mode intensity over all possible excited states of the nucleus in the second well.

Within the one-dimensional model of the potential barrier, the fragmentation effects can be taken into account by introducing a corresponding imaginary component into the potential $V(\beta)$. This treatment is similar to the consideration of inelastic scattering effects in the optical model. If the imaginary part of the potential is rather small ($\varphi_i << 1$), the energy dependence of the penetrability contains the same resonance structure as in (94), but its maximum values for resonances decrease strongly. In this case the extreme values of the penetrability of the two-hump barrier are described by the relations

$$T_{\max}(E) = \frac{T_A T_B}{(T_A + T_B + T_2)\varphi_i} \quad , \tag{5.7}$$

$$T_{\min}(E) = \frac{T_A T_B}{T_A + T_B + T_2}\varphi_i \quad ,$$

where T_2 is the transmission coefficient for the gamma-ray decay in the second well. The average penetrability $P(E)$ remains, however, the same as without the imaginary component that simulates the dissipation of the vibrational excitations.

At large φ_i the coefficient of transition through the two-hump barrier has the following form

$$T(E) = \frac{T_A T_B}{T_A + T_B + T_2} \quad . \tag{5.8}$$

This case corresponds to the total break-down of the vibrational states in the second well into states of a intrinsic nature. The transition through the barrier in this case is determined by the probability of sequential transitions through each of the humps. If $T_2 << (T_A + T_B)$, the probability of the transition through the asymmetric two-hump barrier will be the same as that of one-hump barrier, equivalent to the higher hump.

The above equations show that the energy dependence of fission widths in the two-hump model is much more complicated than for the one-hump barrier. The quasi-stationary states of the nucleus in the well between the humps modulate the penetrability of the barrier. These modulations are revealed in the cross-section of the sub-barrier fission of nuclei in the form of different intermediate structures. The above model of a complex one-dimension barrier determines the penetrability averaged over the spectrum of multiparticle excitations of the nucleus in the second well. In case the quasi-stationary levels corresponding to these excitations do not yet overlap, the energy dependence of the penetrability of the two-hump barrier and, consequently, the fission cross-sections should reveal two types of intermediate structures: a gross structure resulting from the vibrational states of the nucleus in the well between the humps, and a smaller structure related to various excitations of other degrees of freedom of the nucleus. The resonances observed in the ^{230}Th(n,f) reaction at neutron energy of about 700 keV [67V] and in the cross-sections of ^{239}Pu(d,pf) reaction at the excitation energy of the fissioning nucleus of about 5 MeV [69P] can

serve as most vivid examples. The other type of an intermediate structure is demonstrated in the cross-sections of ^{240}Pu fission by resonance neutrons [68M]. The quantitative analysis of these structures as well as a more detailed discussion of the experimental data obtained and equations of the resonance reactions theory needed for their description are contained in [68L, 80B1].

When discussing different aspects of the two-hump barrier it should be borne in mind that the fundamental postulates of this model are inseparable from the understanding of the governing influence exerted by shell inhomogeneities of the one-particle spectrum on many properties of nuclei. This model helped to explain and systematize numerous experimental data on the fission of actinides. More complete reviews of modern problems of nuclear fission physics may be found in Refs. [73V, 91W].

Conclusion

Only the basic aspects of the statistical theory of nuclear reactions have been discussed in the above lectures. A limited time does not allow to consider such questions as: the preeqilibrium reactions, intermediate at time between the fast direct and the relatively slow compound processes; the damping of collective enhancement of nuclear level densities at high excitation energies; the specific features of fission process related to nuclear viscosity and the corresponding reduction of fission probability at high energies. These questions are rather important for many practical applications and they will be partially discussed by other lectors.

The statistical theory relations are widely utilized in the modern computer programs the most known of which are the GNASH [98Y], EMPIRE [07H], and TALYS [07K] codes. Two last codes will be discussed at the present Workshop in details together with the corresponding excesses. Advanced modeling codes require a considerable amount of numerical input, therefore the International Atomic Energy Agency has worked extensively during the last 15 years to prepare a library of validated nuclear-mode input parameters, referred as the Reference Input Parameter Library (RIPL) [98O, 06B, 09C]. Main components this library will be discussed in the next lecture.

References

35A Amaldi, E., D'Agostino, I., Fermi, E., et al.: Proc. Roy. Soc. **A149** (1935) 522
36B1 Bohr, N.: Nature **137 (**1936) 344
36B2 Breit, G., Wigner, E.P.: Phys. Rev. **49** (1936) 519
37B Bethe H. Rev. Mod. Phys. **9** (1937) 69
38K Kapur, P.L., Peierls, D.E.: Proc. Roy. Soc. **A166** (1938) 277
39B Bohr, N, Wheeler, J.A.: Phys. Rev. **56** (1939) 426
39F Frenkel, Ya.I.: JETP **9** (1939) 641
39L Lamb, W.E.: Phys. Rev. **55** (1939) 190
47W Wigner, E.P., Eisenbud L.: Phys.Rev. **72 (**1947) 29
49F Fernbach H., Sorber R., Taylor T.: Phys. Rev. **75** (1949) 1352
51W1 Wigner, E.P.: Ann. Math. **51** (1951) 36; **62**(1955)548; **65** (1957) 203; **67** (1958) 325
51W2 Wolfenstein, L.: Phys. Rev. **82** (1951) 690
52B1 Barschall, H.: Phys. Rev. **86** (1952) 431
52B2 Blatt, J.M., Weisskopf, V.F.: *Theoretical Nuclear Physics*, Wiley, NY, 1952
52H Hauser, W., Feshbach H.: Phys. Rev. **87** (1952) 366
54F Feshbach, H., Porter, C.E., Weiskopf V.F.: Phys. Rev. **96** (1954) 448
54L Lang J.M., Le Couteur K.J. *Proc. Phys. Soc.,* **A67** (1954) 586
55B1 Bohr, A., in: First Conf. on Peaceful Uses of Atomic Energy (Geneva 1955), United Nations, NY, **2** (1955) 151
55B2 Brink, D..M.: PhD Thesis, Oxford Univeraty, 1955
55F Friedman, F.L., Weisskopf, V.F. in: Niels Bohr and the Development of Physics. Ed. W.Pauli, Pergamon, NY, 1955, p. 134
55G Ghiorso, A., et al.: Phys. Rev. **98** (1955) 1518; **99** (1955) 1048
56P Porter, C.E., Thomas, R.G.: Phys. Rev. **104** (1956) 483
57L Landau, L.D.: JETP **32** (1957) 59

57M Margolis, B., Trubezkoy E.S.: Phys. Rev. **106** (1957) 105
58E Ericson, T., Strutinski, V.M.: Nucl. Phys. **8** (1958) 481
58C Chase, D., Wilets, L., Edmonds, A.R.: Phys. Rev. **110** (1958) 1080
58F1 Feshbach, H.: Ann. Phys. **5** (1958) 357
58F2 Flerov, G.N., in: : Second Conf. on Peaceful Uses of Atomic Energy, United Nations, Geneva, **14** (1958) 151
58G Groshev, L.V., et al., in: Second Conf. on Peaceful Uses of Atomic Energy, United Nations, Geneva, **15** (1958) 138
58L Lane, A.M., Thomas, R.G.: Rev. Mod. Phys. **30** (1958) 257
58V Vladimirsky, V.V, Il'yna I.L.: Nucl. Phys. **6** (1958) 235
59I Igo, G.: Phys. Rev. **115** (1959) 1665
60B Bilpuch E.G., Weston L.W., Newson H.W.: Ann. Phys. 10 (1960) 455
60E Ericson, T.: Adv. Phys. **9** (1960) 425
60L Lane, A.M., Lynn, J.R.: Nucl. Phys. **17** (1960) 553
60N Nemirovski, P.I.: *Modern Nuclear Models*. Atomizdat, Moscow, 1960
61E Erba E., Facchini U., Saetta-Menicella. *Nuovo Cim.* **22** (1961) 1237
61W Wilkinson, D., in: Nuclear Spectroscopy. Academic Press, NY, London, 1961, p. 852
62A Axel, P.: Phys. Rev. **126** (1962) 671
62D Dyson, F.J.: J. Math. Phys. **3** (1962) 140, 157, 166, 1191, 1199
62P Polikanov, S.M., et al.: JETP **42** (1962) 1464
63H Hodson, P.E.: *Optical Model of Elastic Scattering*, Oxford Press, 1963
65G Gilbert A., Cameron A. *Can. J. Phys.* **43** (1965) 1446
64M Moldauer, P.A.: Phys. Rev. **135B** (1964) 642; Rev. Mod. Phys. **36** (1964) 1079
65P Porter, C.E. (ed.): Statistical Theories of Spectra. Academic Press, NY, 1965
65T Tamura, T.: Rev. Mod. Phys. **37** (1965) 579
66S Strutinsky, V.M.: Sov. J. Nucl. Phys. **3** (1966) 449; Nucl. Phys. **A95** (1967) 420
67M1 Mehta, M.L.: *Random Matrics*. Academic Press, NY, 1967
67M2 Moldauer, P.A.: Phys. Rev. **157** (1967) 907
67MS Myers W.D., Swiatecki W.J. *Ark. Fysik*, **36** (1967) 593
67V Vorotnikov, P.E., et al.: Sov. J. Nucl. Phys. **5** (1967) 210
68L Lynn, J.R.: *Theory of Neutron Resonance Reactions*. Clarendon Press, Oxford, 1968
68M Migneko, E., Theobald, J.P.: Nucl. Phys. **A112** (1968) 603
68S Strutinsky, V.M.: Nucl. Phys. **A122** (1968) 1
69B Bjornholn, S., Strutinsky, V.M.: Nucl. Phys. **A136** (1969) 1
69C Chrien, R.E., in: Proc. Symp. on Neutron Capture γ-ray Spectroscopy. Studsvic, 1969, p. 62
69I Ignatyuk, A.V., Rabotnov, N.S., Smirenkin, G.N.: Phys. Lett. **B29** (1969) 209
69M Malyshev A.V. *Level Density and Structure of Atomic Nuclei (Rassian).* Atomizdat, M., 1969.
69P Pedersen, J., Kuzminov, B.D.: Phys. Lett. **B29** (1969) 176
70A Austern, N.: *Direct Nuclear Reaction Theories*. Wiley, NY, 1970
70B Bollinger, L.M., Thomas, G.R.: Phys. Rev. **C2** (1970) 1271
70I Ignatyuk, A.V., Stavinsky, V.S., Shubin, Yu.N. in: Nucl. Data for Reactors, IAEA, Vienna, 1970, v.2, p. 885
70R Ramamurthy, V.S., Kapoor S.S., Kataria S.K. Phys. Rev. Lett. **25** (1970) 386
70S Stavissky, Yu.Ya, et al.: *Radiative capture of fast neutrons*, M., Atomizdat, 1970.
71C Carlos, P., et al.: Nucl. Phys. **A172** (1971) 437
71L Lane, A.M.: Ann. Phys. **63** (1971) 340
71M Mughabghab S.F., et al.: Phys. Rev. Lett. **26** (1971) 1118
71W Wilhelm, I., et al.: Izv. AN SSSR, Ser. Fiz. **35** (1971) 1542
72B Bollinger, L.M.: Sov. Part. Nucl. **2** (1972) 188
72C Camarda, H.S., et al., in: Statistical Properties of Nuclei, J.B.Card (ed.), Plenum Press, NY, 1972, p. 285
72L Liou, H.I, Camarda, H.S., Rahn, F.: Phys. Rev. **C5** (1972) 1002
72N Newsted, C.M., Delaroche, J., Canvin, B. in: Statistical Properties of Nuclei, J.B.Card (ed.), Plenum Press, NY, 1972, p. 367
72P1 Pasechnik, M.V., Korzh, I.A., Koshuba, I.E. in: Neutron Physics, Naukova Dumka, Kiev, 1972, Vol. 1, p. 403
72P2 Popov, Yu.P., et al.: Nucl. Phys. **A188** (1972) 212

73D Dilg W., Schantl W., Vonach H., Uhl M. *Nucl. Phys.,* **A217**, 269 (1973).
73H Holmqvist, B., Wiedling, T.: J. Nucl. Energy **27** (1973) 543
73V Vandenbosh, R., Huizenga J.R.: Nuclear Fission, Academic Press, NY, 1973
74B Bartholomew, G.A., et al.: Adv. Nucl. Phys. **7** (1974) 229
74BM Bohr A., Mottelson B. *Nuclear Strucrure.* Benjamin Inc., NY-Amsterdam, 1974, v.2.
74F Feshbach, H.: Rev. Mod. Phys. **46** (1974) 1
74L Lane, A.M., Mughabghab, S.F.: Phys. Rev. **C10** (1974) 412
74T Tepel, J.W., Hoffman, H.M., Weidenmuller, H.: Phys. Lett. **B49** (1974) 1
74W Weidenmuller, H.: Phys. Rev. **C9** (1974) 1202
75A Agassi, G., Weidenmuller, H., Mantzouranis, G.: Phys. Rep. **C22** (1975) 14
75B1 Barrett, R.F.,Teresawa, T.: Nucl.Phys. **A240** (1975) 445
75B2 Bohigas, O., Giannoni, M.J.: Ann. Phys. **86** (1975) 921
75C Cugnon, J., Mahaux, C.: Ann. Phys. **94** (1975) 128
75H Hoffman, H.M., Richter, J., Tepel, J.W., Weidenmuller, H.: Ann. Phys. **9** (1975) 403
75IS Ignatyuk A.V., Smirenkin G.N., Tishin A.S.: *J. Sov. Nucl. Phys*. **21** (1975) 255
75K Kadmenski, S.G., Furman, V.I.: Sov. Part. Nucl. **6** (1975) 189
75M Moldauer, P.A.: Phys. Rev. **C11** (1975) 426; **C12** (1975) 744
75P Popov, Yu.P., in: Neutron Capture Gamma-Ray Spectroscopy, RCN, Petten, 1975, p.379
75T Tanaka S., in: Proc. EANDC Topical Discussion, JAERI-5984, 1975, p. 212
76C Cullen, D.E., Weisbin, C.R.: Nucl. Sci. Eng. **60** (1976) 199
77J Johnson, C.H.: Phys. Rev. **C16** (1977) 2238
77U Urin, M.G.: Sov. Part. Nucl. **8** (1977) 817
78A Allen, B.J., Musgrove, A.R., in: Adv. Nucl. Phys. **10** (1978) 129
78K Kataria S.K., Ramamurthy V.S., Kapoor S.S. *Phys. Rev.*, **C18** (1978) 549
78M Mughabghab, S.F., in: 3rd School on Neutron Physics (Alushta, 1978), Dubna, JINR, 1978, p. 328
78S Soloviev, V.G.: Sov. Part. Nucl. **9** (1978) 580
79I Ignatyuk A.V., Istekov K.K., Smirenkin G.N.: *Sov. Nucl. Phys.,* **29** (1979) 450
79M1 Mughabghab, S.F.: Phys. Lett. **B81** (1979) 93
79M2 Mughabghab, S.F., Olden, R.E., in: Neutron Capture Gamma-Ray Spectroscopy, Plenum Press, NY,1979, p. 266
79S Soloviev, V.G., Stoyanov, Ch., in: Neutron Capture Gamma-Ray Spectroscopy, Plenum Press, NY, 1979, p. 145
80B1 Bechvarzh, F., in: Nuclear Structure, Dubna, JINR, 1980, p. 31
80B2 Bjornholn, S., Lynn, J.R.: Rev. Mod. Phys. **52** (1980) 725
80F Feshbach, H.: Ann. Phys. **125** (1980) 429
80I Ignatyuk A.V., Istekov K.K., Okolovich V.N., Smirenkin G.N. In: Physics and Chemistry of Fission, IAEA, Vienna, 1980, v. 1, p. 21.
80M Moor, M.S., in: Nuclear Theory for Applications, Trieste, IAEA-SMR-43, 1980, p. 31
80R Raman S., et al.: Phys. Rev. **C22** (1980) 328
81B Brody, T.A., et al.: Rev. Mod. Phys. **53** (1981) 385
81C Chrien, R.E, McCullgh, C., Stelts, M.L.: Phys. Rev. **C23** (1981) 1394
81M Mughabghab, S.F., Divadeenam, M., Holden, N.E.: Neutron Cross Sections, v. 1, part. A, Academic Press, New York, 1981
82B Bondarenko, V.I., Urin, M.G.: Sov. J. Nucl. Phys **35** (1982) 245
82H Hardy, J.C.: Phys. Lett. **B109** (1982) 242
82R Raman, S., in: Neutron Capture Gamma-Ray Spectroscopy and Related Topics, Bristol, London: Inst. Phys. Conf. Ser, 1982, p. 357
82K Kadmenski, S.G., Kurgalin, S.D., Furman, V.I.: Sov. J. Nucl. Phys. **35** (1982) 479
82P Popov, Yu.P., in: Neutron Induced Reactions, P. Oblozinsky (ed.), Bratislava, SAS, 1982, p. 121
83A Allen, B.J., in: Nuclear Data for Science and Technology, K.H. Bockhoff (ed.), Brussels, Luxemburg, ECSC, 1983, p. 707
83B Bychkov, V.M., et l.: Sov. J. Part. Nucl. **14** (1983) 373
83F Flerov, G.N., Ter-Akopian, G.M.: Sov. Part. Nucl. **46** (1983) 817
83I A.V.Ignatyuk: *Statistical Properties of Excited Atomic Nuclei (Russian)*, Energoatomizdat, Moscow, 1983; Translated by IAEA, *Report INDC-233(L),* Vienna, 1983.
83K Kadmenski, S.G., Markushev, V.N., Furman V.I.: Sov. J. Nucl. Phys. **37** (1983) 165
83M Malecky, H., Popov, A.B., Tshezak, K.: Sov. J. Nucl. Phys. **37** (1983) 169
83S Satchler, G.R.: *Direct Nuclear Reactions,* Oxford Press, 1983.

84M Mughabghab, S.F.: *Neutron Cross Sections*, Vol. 1, part B, New York: Academic Press, 1984
84U Urin, M.G.: Sov. Part. Nucl. **15** (1984) 245
85K Kadmenski, S.G., Furman, V.I.: *Alpha-radioactivity*, Energoatomizdat, Moscow, 1985
86B Belanova, T.S., Ignatyuk, A.V., Pashchenko, B.I., Plyaskin, V.I.: *Radiative Neutron Capture Handbook (Russian)*, Energoatomizdat, Moscow, 1986.
86C Chrien, R.E., in: 5th School on Neutron Physics (Alushta 1986), Dubna, JINR, 1986, p.29
86R Raman, S., Lynn, J.E., in: Neutron Induced Reactions (Smolenice 1985), J.Kristiak, E.Betak (eds.), Bratislava, VEDA, 1986, p.253
90B Balabanov N.P., Vtyurin V.A., Gledenov Yu.M., Popov Yu.P.: Sov. J. Part. Nucl. **21** (1990) 131
90K Kopecky, J., Uhl, M.: Phys. Rev. **C41** (1990) 1941
90S Seaborg, G.T., Loveland, W.D.: *Elements beyond Uranium,* Wiley, NY, 1990
91W Wagemans, C. (ed.): Nuclear Fission Process, CRC Press, Boca Raton, 1991
94M Mengoni A., Nakajima Y.: *J. Nucl. Sci. Tech.,* **31** (1994) 151
98O Oblozinsky, P., Chadwick, M.B., Fukahori, T. et al.: *Handbook for Calculations of Nuclear Reaction Data: Reference Input Parameter Library*, IAEA-TECDOC-1034, IAEA, Vienna, 1998; (see http://www-nds.iaea.org/ripl/).
98Y Young, P.G., Arthur, E.D., and Chadwick, M.B.: in: Nuclear Reaction Data and Nuclear Reactors, A.Gandini, G.Reffo (eds.), Singapore, World Sci., 1998, vol. 1, p. 227
06B Belgya, T., Bersillon, O., Capote R. et al.: *Handbook for calculations of nuclear reaction data, Reference Input Parameter Library RIPL-2*, IAEA-TECDOC-1506, IAEA, Vienna, 2006; (see http://www-nds.iaea.org/RIPL-2/)
07H Herman, M., Capote, R., Carlson, B.V., et al.: Nucl. Data Sheets. **108**, (2007) 2655
07K Koning, A.J., Hilaire, S., and Duijvestijn, M.: *TALYS-1.0: A Nuclear Reaction Program (User Manual)*, NRG/CEA, 2007
09C Capote, R., Herman, M., Oblozinsky, P., et al.: Nucl. Data Sheets. **110**, (2009) 3107 (see http://www-nds.iaea.org/RIPL-3/)